

---

# Relational In-Context Learning via Synthetic Pre-training with Structural Prior

---

Yanbo Wang<sup>1</sup> Jiaxuan You<sup>2</sup> Chuan Shi<sup>3</sup> Muhan Zhang<sup>1</sup>

## Abstract

Relational Databases (RDBs) are the backbone of modern business, yet they lack foundation models comparable to those in text or vision. A key obstacle is that high-quality RDBs are private, scarce and structurally heterogeneous, making internet-scale pre-training infeasible. To overcome this data scarcity, We introduce **RDB-PFN**, the first relational foundation model trained purely via **synthetic data**. Inspired by Prior-Data Fitted Networks (PFNs) where synthetic data generated from Structural Causal Models (SCMs) enables reasoning on single tables, we design a **Relational Prior Generator** to create an infinite stream of diverse RDBs from scratch. Pre-training on **over 2 million** synthetic single-table and relational tasks, RDB-PFN learns to adapt to any new database instantly via genuine **in-context learning**. Experiments verify RDB-PFN achieves strong few-shot performance on 19 real-world relational prediction tasks, outperforming graph-based and single-table foundation-model baselines (given the same DFS-linearized inputs), while using a lightweight architecture and fast inference. The code is available at <https://github.com/MuLabPKU/RDBPFN>.

## 1. Introduction

**The Foundation Model Discrepancy.** Relational Databases (RDBs) serve as the bedrock of modern enterprise, storing the vast majority of the world’s high-value structured data (Codd, 1970; 2007; Harrington, 2016). Yet, a stark discrepancy defines the current AI landscape: while Foundation Models (FMs) have revolutionized unstructured modalities like text and vision through massive scale (Brown et al., 2020; Achiam et al., 2023; Dosovitskiy, 2020), RDBs remain largely untouched by this paradigm shift. In the RDB domain, the standard workflow still relies on be-

spoke feature engineering followed by single-table methods like Gradient Boosted Decision Trees (GBDTs) (Chen, 2016; Prokhorenkova et al., 2018; Ke et al., 2017), or task-specific architecture search using Graph Neural Networks (GNNs) (Wang et al., 2024; Robinson et al., 2024).

**The Data Wall.** The primary bottleneck preventing foundation models for RDBs is not architectural, but data-centric. Foundation models in NLP and Vision rely on the “Scaling Law”, the emergence of reasoning capabilities from massive ingestion of public real-world data (Kaplan et al., 2020). For RDBs, this approach fails because high-quality corporate databases are inherently private, scarce, and structurally heterogeneous (Wang et al., 2024), rendering the standard pre-training methodology infeasible. Recent attempts on RDB foundation models, such as Griffin (Wang et al., 2025) and RT (Ranjan et al., 2025), rely on limited open-sourced repositories of real-world data, which is far from the pre-training scale. Consequently, they fail to achieve universal generalization without fine-tuning.

**The PFN Insight: Learning from Synthetic Data.** To circumvent this fundamental data scarcity, we turn to the emerging paradigm of **Prior-Data Fitted Networks (PFNs)** (Müller et al., 2021). PFNs leverage a counter-intuitive strategy: instead of training on scarce real-world data, they learn to approximate Bayesian Inference by pre-training on a vast corpus of synthetic tasks generated from Structural Causal Models (SCM). The core mechanism relies on the Transformer’s ability to act as a “learning algorithm”: by attending to the context of synthetic examples, the model learns to simulate the posterior predictive distribution. As long as the statistical structure of the real world falls within the support of this synthetic prior, the model generalizes automatically. This methodology has revolutionized the single-table domain: **TabPFN** (Hollmann et al., 2022) demonstrated that a Transformer trained purely on synthetic priors could outperform tuned GBDTs on small datasets. Crucially, it achieves this with an over  $5,000\times$  speedup, replacing iterative training with a single forward pass that performs In-Context Learning (ICL). Subsequent work continues to scale and refine this paradigm, shifting the core challenge from intractable data collection to solvable prior design—enabling models to generalize to entirely new schemas without a single gradient update.

<sup>1</sup>Institute for Artificial Intelligence, Peking University  
<sup>2</sup>University of Illinois at Urbana-Champaign <sup>3</sup>Institute of Computing Technology, Beijing University of Post and Telecommunication. Correspondence to: Muhan Zhang <muhan@pku.edu.cn>.

**The Relational Gap.** However, the success of PFNs has essentially been confined to the single-table setting, where the prior typically assumes rows are Independent and Identically Distributed. This assumption violates the core of relational data. As highlighted by RDB benchmarks like 4DBInfer (Wang et al., 2024) and Relbench (Robinson et al., 2024), RDBs are defined by *interconnectivity*: a label in a “User” table is not merely a function of user attributes, but is often a complex aggregation of historical records in “Order” or “Click” tables. Applying standard single-table generators to RDBs fails to model these interactions. The field lacks a **Relational Prior**: a generative framework capable of synthesizing valid schema topologies, foreign key dependencies, and causal aggregations from scratch.

**Our Approach: RDB-PFN.** In this work, we introduce RDB-PFN, the first RDB foundation model built on a relational prior and pretrained purely on synthetic data. We formalize a novel generative mechanism that samples infinite streams of random schema topologies and propagates causal signals within and across tables. We prove a universality result under acyclic-schema, local Markov, and conditional-exchangeability assumptions. Based on synthetic RDBs sampled from our prior, we employ a rigorous curriculum, pre-training the model on over 2 million synthetic tasks. To isolate the importance of our relational prior, we pair this sophisticated data generation with a simple “Linearize-and-Attend” architecture, using standard Deep Feature Synthesis (DFS) (Kanter & Veeramachaneni, 2015) and a vanilla Transformer. This demonstrates that the model’s relational intelligence stems from the prior’s design rather than architectural complexity.

We extensively evaluated RDB-PFN on 19 real-world relational learning tasks. The results confirm that our approach delivers superior performance and efficiency: RDB-PFN outperforms both traditional GBDT baselines and general tabular foundation models in the few-shot regime, while requiring significantly fewer **parameters**, faster **inference speeds**, and orders of magnitude less **pre-training data**.

Our core contributions are summarized as follows:

- **Solving Scarcity via Synthetic Data:** Unlike traditional relational learning methods that require expensive fine-tuning on target tasks or pre-training on sensitive real-world data, RDB-PFN is trained **purely on synthetic data**. It performs **zero-gradient** inference strictly via ICL, effectively eliminating the dependency on large real-world datasets for both pre-training and adaptation.
- **Prior > Scale:** When compared to state-of-the-art Single-Table Foundation Models (augmented with DFS), RDB-PFN exceeds their performance despite using a fraction of the model size and training compute. This confirms that pre-training on a physically consistent **Relational Prior** equips the model with a structural inductive bias

that cannot be efficiently replicated simply by scaling up generic tabular data.

## 2. Related Work

### 2.1. From Tabular to Relational Learning

Prior to the Foundation Model era, standard approaches required training models from scratch for each specific dataset.

**Single-Table Baselines.** Research on single table data has evolved through various approaches. Traditional methods, such as XGBoost (Chen, 2016), LightGBM (Ke et al., 2017), and CatBoost (Prokhorenkova et al., 2018), have been widely adopted due to their scalability. More recently, transformer-based methods like TabTransformer (Huang et al., 2020), TabNet (Arik & Pfister, 2021), FT-Transformer (Gorishniy et al., 2021), and SAINT (Somepalli et al., 2021) have leveraged attention mechanisms to capture complex relationships. Additionally, graph-based methods such as GRAPE (You et al., 2020), TabularNet (Du et al., 2021), TabGNN (Guo et al., 2021), and CARTE (Kim et al., 2024) represent tabular data as graphs to model interactions more effectively. Recent advancements have expanded beyond general architecture search to focus on refining specific components of the tabular modeling pipeline. Significant progress has been made in numerical encoding strategies (Gorishniy et al., 2022; Yarullin & Isaev, 2023), retrieval-augmented modeling that incorporates nearest-neighbor context (e.g., TabR (Gorishniy et al., 2023), ModernNCA (Ye et al., 2025)), and robust training protocols such as default-pre-tuning (RealMLP (Holzmüller et al., 2024)) or efficient ensembling (TabM (Gorishniy et al., 2024)). However, despite these innovations, they inherently assume a linearized feature vector and lack native mechanisms to capture the complex, multi-table topology of relational databases.

**The Relational Bridge: RDB Models.** RDBs extend the concept of single-table models by incorporating multiple interrelated tables, requiring models to capture both intra- and inter-table relationships. Early approaches, such as DFS (Kanter & Veeramachaneni, 2015) and RDB2Graph (Cvitkovic, 2020), attempted to flatten RDBs into a single table or apply GNNs to model relationships. Other works, like ATJ-Net (Bai et al., 2021) and KEN (Cvetkov-Iliev et al., 2023), use hypergraphs and knowledge graphs to model inter-table dependencies, while GFS (Zhang et al., 2023) integrates differentiable single-table models as embedding functions to preserve table structures. Some methods convert structured data into unstructured embeddings while retaining structural information (Grover & Leskovec, 2016), such as EmbDi (Cappuzzo et al., 2020) and RDF2Vec (Ristoski & Paulheim, 2016).

As RDB tasks have attracted increasing attention (Fey et al.,

2024), more comprehensive benchmarks and toolboxes have emerged. For example, 4DBInfer (Wang et al., 2024), Rel-Bench (Robinson et al., 2024; Fey et al., 2023), and PytorchFrame (Hu et al., 2024) propose complete pipelines for converting RDBs into graph structures for GNN-based models. More recent efforts, such as ContextGNN (Yuan et al., 2024), RelGNN (Chen et al., 2025) and RelGT (Dwivedi et al., 2025), aim to design more expressive GNN architectures specifically for relational data. However, these models are still limited on individual RDB tasks.

## 2.2. Foundation Models for Structured Data

While language and vision fields have achieved scalability through massive real-world data ingestion, the structured data domain is still in search of a unified paradigm.

**Single-Table Landscape: Real vs. Synthetic.** Early attempts at tabular foundation models relied on large-scale real-world corpora, employing supervised or masked self-supervised learning (Zhu et al., 2023; Wang & Sun, 2022; Yang et al., 2023; Kim et al., 2024). However, these efforts struggled to generalize due to the lack of shared semantics across diverse tables. A paradigm shift occurred with Prior-Data Fitted Networks (PFNs) (Müller et al., 2021). TabPFN (Hollmann et al., 2022; 2025) demonstrated that training on synthetic datasets generated from Structural Causal Models allows a model to approximate Bayesian Inference, achieving state-of-the-art few-shot performance without observing real-world data—a result verified by numerous follow-up studies (Grinsztajn et al., 2025; Qu et al., 2025; Zhang et al., 2025a;b). This synthetic paradigm is now rapidly expanding to other domains, including time-series (Taga et al., 2025; Dooley et al., 2023; Hoo et al., 2025), causal discovery (Robertson et al., 2025; Balazadeh et al., 2025; Ma et al., 2025), and graph learning (Eremeev et al., 2025b;a; Hayler et al., 2025), among others.

**The Relational Gap.** Despite the success of PFNs in the single-table domain, relational modeling remains tied to the traditional Pre-training & Fine-tuning paradigm. Recent efforts like Griffin (Wang et al., 2025) and RT (Ranjan et al., 2025) rely on aggregating limited real-world repositories, employing text unification strategies and incorporating auxiliary tables. While valuable, these methods are fundamentally constrained by the scarcity of public schemas where they focus gradient-based fine-tuning to adapt to new tasks. To date, the field lacks a genuine foundation model.

## 2.3. Generative Models for Relational Databases

Existing research on RDB generation focuses mainly on *Privacy-Preserving Data Publishing*. The primary objective is to train a model on a specific private database ( $D_{real}$ ) to produce a high-fidelity synthetic replica ( $D_{syn}$ ).

**From Statistics to Powerful Generation Models.** Early

approaches like SDV (Patki et al., 2016) and RC-TGAN (Guye et al., 2023) relied on statistical copulas or GANs to clone parent-child relationships. Recently, the state-of-the-art has shifted toward **Graph-Conditional Diffusion**. Models such as ClavaDDPM (Pang et al., 2024), RelDiff (Hudovernik et al., 2025), and GRDM (Ketata et al., 2025) achieve superior fidelity by treating the database as a joint distribution and utilizing GNNs to iteratively denoise complex schemas.

**Incompatibility with Foundation Models.** However, these methods are not suitable for pre-training Foundation Models. First, as *Conditional Generators*, they depend on real input data, creating a circular dependency that fails to address the fundamental scarcity of RDBs. Second, their iterative sampling processes (e.g., diffusion denoising) are prohibitively slow for the high-throughput generation required to train on millions of tasks. To overcome this, we require an **Unconditional Relational Prior** capable of generating complex RDBs purely from scratch at scale.

**Positioning.** Our work differs from prior RDB models (e.g., GNN-based architectures and fine-tuned relational pre-training) in that RDB-PFN is trained primarily on *synthetic relational databases* generated from an *unconditional relational prior* and performs inference via *in-context learning* without gradient updates. It also differs from privacy-focused relational data generators, which are conditional models trained to clone a specific private database and are not designed for high-throughput task generation for foundation-model pre-training.

## 3. Preliminaries

**Definition 3.1** (Relational Database: Schema and Instance). A RDB is specified by a **schema** and a **populated instance**.

**Schema.** The schema is a collection of tables  $\mathcal{T} = \{T_1, \dots, T_N\}$ . Each table  $T$  has a set of columns  $\mathcal{C}(T) = \mathcal{K}^{pk}(T) \cup \mathcal{K}^{fk}(T) \cup \mathcal{A}(T)$ , where  $\mathcal{K}^{pk}(T)$  are **primary key (PK)** columns,  $\mathcal{K}^{fk}(T)$  are **foreign key (FK)** columns, and  $\mathcal{A}(T)$  are all remaining **feature columns**. Each FK column  $k \in \mathcal{K}^{fk}(T)$  references a *parent table*  $\text{Ref}(k) \in \mathcal{T}$ .

**Instance.** A database instance  $\mathcal{D}$  assigns concrete rows to each table. Let  $\mathcal{V}(T)$  denote the set of rows in table  $T$ ; each row is a record containing values for all columns in  $\mathcal{C}(T)$ . PK values uniquely identify rows within a table, and FK values must match PK values in the referenced parent table.

**Definition 3.2** (Source vs. Dependent Tables). A table  $T$  is a **source table** if it has no foreign keys, i.e.,  $\mathcal{K}^{fk}(T) = \emptyset$ . A table  $T$  is a **dependent table** if it has one or more foreign keys, i.e.,  $\mathcal{K}^{fk}(T) \neq \emptyset$ .

**Definition 3.3** (Schema Graph and Instance Graph). We use two levels of topology.

**Schema graph.** The schema graph is a directed graph  $G_S = (\mathcal{V}_S, \mathcal{E}_S)$  with nodes  $\mathcal{V}_S = \mathcal{T}$ . We orient edges as **parent**  $\rightarrow$  **child**:

$$(T_p \rightarrow T_c) \in \mathcal{E}_S \iff \exists k \in \mathcal{K}^{fk}(T_c) \text{ s.t. } \text{Ref}(k) = T_p.$$

**Instance graph.** The instance graph is a directed graph  $G_{in} = (\mathcal{V}_{in}, \mathcal{E}_{in})$  whose nodes are **rows**:  $\mathcal{V}_{in} = \bigcup_{T \in \mathcal{T}} \mathcal{V}(T)$ . For a row  $u \in \mathcal{V}(T)$ , let  $\text{pk}(u)$  denote its (possibly composite) primary-key value. For a foreign-key column  $k \in \mathcal{K}^{fk}(T_c)$  and a child row  $v \in \mathcal{V}(T_c)$ , let  $\text{fk}_k(v)$  denote the value stored in column  $k$  of row  $v$ . We orient edges consistently as **parent row**  $\rightarrow$  **child row**:

$$(u \rightarrow v) \in \mathcal{E}_{in} \iff v \in \mathcal{V}(T_c), u \in \mathcal{V}(T_p), \\ \exists k \in \mathcal{K}^{fk}(T_c) \text{ s.t. } \text{Ref}(k) = T_p \wedge \text{fk}_k(v) = \text{pk}(u).$$

We optionally associate each row-node  $r$  in the instance graph  $G_{in}$  with a latent structural state  $Z_r \in \mathbb{R}^d$ , and denote the collection by  $\mathcal{Z} := \{Z_r\}_{r \in \mathcal{V}_{in}}$ .

**Definition 3.4** (Relation Types and Neighborhoods). Each FK type induces a **relation type**  $\tau$  (e.g.,  $T_p \rightarrow T_c$ ), and we also consider its reverse relation  $\tau^{-1}$  to enable bidirectional message passing. For a row-node  $v \in \mathcal{V}_{in}$ , let  $\mathcal{R}(v)$  be the set of relation types incident to  $v$ . For a relation type  $\tau$ , let  $\mathcal{N}_\tau(v)$  denote the neighbor set of  $v$  under  $\tau$  (parents for  $\tau$  pointing into  $v$ , children for  $\tau$  pointing out of  $v$ , depending on the chosen direction).

**Definition 3.5** (Relational Prediction Task and In-Context Learning). A relational prediction task selects a **target table**  $T_\star$  and a **target column**  $y \in \mathcal{A}(T_\star)$  (could be computed via SQL Query). Each target row  $v \in \mathcal{V}(T_\star)$  is mapped to a fixed-length feature vector  $x_v$  by a deterministic linearization operator (e.g., DFS) applied to the database instance:

$$X = \text{Linearize}(\mathcal{D}, T_\star) \in \mathbb{R}^{|\mathcal{V}(T_\star)| \times p},$$

where each row of  $X$  corresponds to one  $v \in \mathcal{V}(T_\star)$  and  $p$  is the standardized feature width.

In the ICL setting, we form a context set  $\mathcal{D}_{ctx} = \{(x_i, y_i)\}_{i=1}^n$  from labeled rows of  $T_\star$  and predict the label of a query row  $(x_q, y_q)$  via a single forward pass:

$$P_\theta(y_q | x_q, \mathcal{D}_{ctx}).$$

## 4. Design Principles of Relational Prior

The efficacy of a foundation model depends on its exposure to vast and diverse datasets. To achieve this in the relational domain, we seek a *universal prior within a well-defined family* of relational database distributions: one that can synthesize diverse, logically consistent RDBs while remaining tractable to learn and sample from. However, the

combinatorial space of “all possible relational databases” is intractable. Just as single-table models rely on structural assumptions (e.g., i.i.d. sampling/exchangeability) to make learning solvable, we introduce a **Relational Inductive Bias**: a small set of structural constraints that reduces the generation space while preserving the complex topological dependencies commonly observed in real-world systems.

### 4.1. Relational Assumptions

To render the generation of complex RDBs tractable, we summarize three core structural principles. These assumptions constrain the generative prior to a family of distributions that remains consistent with relational logic while avoiding the full combinatorial space of arbitrary schemas and instances.

**Assumption 4.1** (Schema Acyclicity). The schema graph  $G_S$  (Definition 3.3), oriented as **parent**  $\rightarrow$  **child**, is a directed acyclic graph (DAG). *Justification*: Many real-world analytic schemas (e.g., star/snowflake designs) are naturally acyclic. In our preprocessing of major benchmarks (e.g., Spider (Yu et al., 2018), 4DBInfer (Wang et al., 2024)), over 95% of schemas are acyclic. Restricting to DAGs also enables efficient topological generation of tables and referential links without deadlock.

**Assumption 4.2** (Relational Markovian Locality). Conditioned on the realized structural skeleton (equivalently, the instance graph  $G_{in}$  and structural row states  $\mathcal{Z}$ ), each generated value is locally determined. Concretely, for any generated attribute value associated with a row  $r$ , its conditional distribution depends only on a bounded-hop neighborhood in  $G_{in}$  (and  $Z_r$ ): there exists a local parent set  $Pa(\cdot)$  contained in a  $k$ -hop neighborhood such that

$$P(\text{value} | \text{rest}) = P(\text{value} | Pa(\text{value}), Z_r).$$

*Justification*: This captures empirical locality in relational systems: an entity’s attributes depend on connected records rather than unrelated entities, enabling tractable generation via local aggregation.

**Assumption 4.3** (Conditional Exchangeability / Mechanism Sharing). Within any table  $T$ , rows are exchangeable conditional on the realized instance graph (and structural states): permuting row identities within  $T$  does not change the joint distribution, provided relational links are permuted consistently. Equivalently, rows of the same table are governed by shared mechanisms that are permutation-invariant to the ordering of neighbor sets.

*Justification*: Row indices carry no semantics; dependence between rows is mediated by relational links, and shared mechanisms enable learning from variable-size sets.

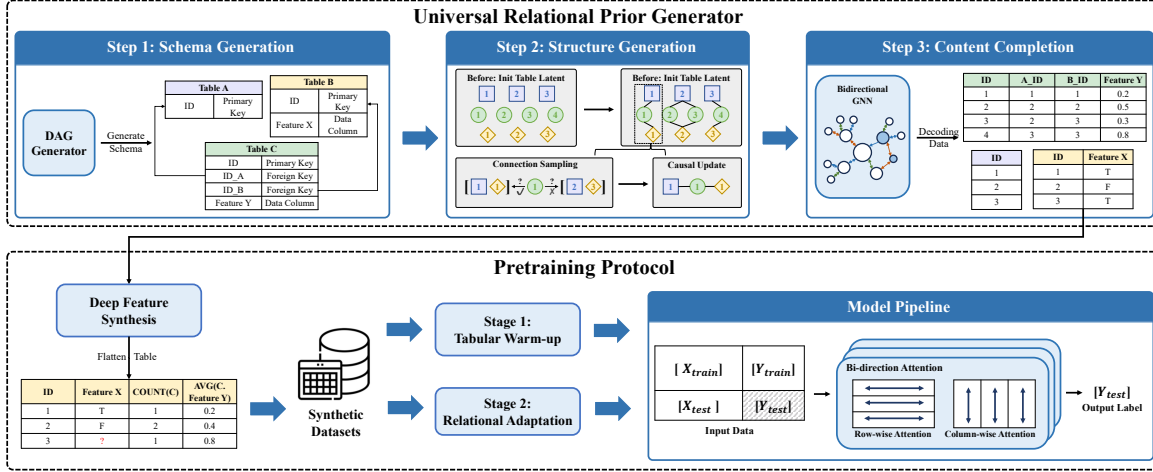


Figure 1. **Overview of the RDB-PFN Framework.** The top panel illustrates our **Universal Relational Prior**, which synthesizes diverse relational databases via a hierarchical decomposition: Schema (LayerDAG), Structure (Hybrid SCM), and Content (Hierarchical SCM). The bottom panel depicts the **Two-Stage Curriculum Learning** protocol, where the model first establishes a statistical backbone on single-table data before adapting to the complex topological signals of linearized relational data.

## 4.2. Constructive Decomposition and Expressivity

Under Assumptions 4.1–4.3, we decompose the database distribution into three stages:

$$P(\mathcal{D}) = \underbrace{P(G_S)}_{\text{Schema}} \cdot \underbrace{P(\mathcal{D}_{struct}, \mathcal{Z} | G_S)}_{\text{Structural Skeleton}} \cdot \underbrace{P(\mathcal{D}_{dep} | \mathcal{D}_{struct}, \mathcal{Z}, G_S)}_{\text{Dependent Content}} \quad (1)$$

where:

- $G_S$  specifies the table-level topology (which tables exist and how they relate).
- $\mathcal{D}_{struct}$  contains all structure-defining fields (PKs, FKs, and any variables used to determine connectivity). They deterministically induce the instance graph  $G_{in}$ .
- $\mathcal{D}_{dep}$  contains remaining attributes generated conditioned on the realized structure, capturing correlations across tables via relational neighborhoods.

**Expressivity (formalized in the appendix).** Eq. equation 1 motivates a modular prior consisting of (i) a schema graph generator, (ii) a structural generator that produces keys/connectivity and optional latent structural states, and (iii) a content generator that fills remaining attributes conditioned on the realized instance graph. In Appendix D (Theorem D.23), we provide a completeness argument showing that, under Assumptions 4.1–4.3 defined high-level relational principles and additional detail assumptions, this composite construction can approximate any target distribution within the resulting assumption-defined family of consistent RDB distributions.

## 5. Method: The RDB-PFN Architecture

We present the practical implementation of the RDB-PFN framework. Our system comprises two components: a scalable **Data Generation Pipeline** and an ICL **Pretraining Pipeline**.

### 5.1. Data Generation

We instantiate the three-stage decomposition (Schema  $\rightarrow$  Structure  $\rightarrow$  Content) using specialized neural modules designed to capture the unique dependencies of each phase.

#### 5.1.1. STAGE 1: SCHEMA GRAPH GENERATION

The first step synthesizes the schema graph  $G_S = (\mathcal{V}_S, \mathcal{E}_S)$ , where nodes are tables and directed edges are oriented as **parent**  $\rightarrow$  **child**. We model the schema distribution  $P(G_S)$  using either (i) **hand-designed topology priors** or (ii) a **learned topology model** trained on *public* schema graphs. In our experiments, we adopt LayerDAG (Li et al., 2024) as a learned schema-topology prior (Appendix C.1.1) to sample realistic DAG topologies. Crucially, regardless of how  $G_S$  is obtained, all table *contents* used for pre-training are generated synthetically by our Stage 2–3 generators.

#### 5.1.2. STAGE 2: STRUCTURAL GENERATION

For **Dependent Tables** (tables referencing  $p$  parent tables), we employ a **Selective SCM** to link each new child row  $v$  to a tuple of existing parent rows  $(u^{(1)}, \dots, u^{(p)})$ .

**1. Latent Initialization:** We first sample a child state  $z_v^{(0)} = \text{MLP}_{init}(\epsilon)$ , representing its latent characteristics.

**2. Connection Sampling via Attention:** We sample  $M$  candidate parent tuples  $C_j = (u_j^{(1)}, \dots, u_j^{(p)})$ , where each  $u_j^{(t)}$  is an existing row from the  $t$ -th parent table. We maintain a

dynamic embedding  $e_u$  for each parent row  $u$  (initialized at creation and optionally updated during generation). Each candidate tuple is embedded as

$$h_{C_j} = \text{MLP}_{comb} \left( e_{u_j^{(1)}} \oplus \dots \oplus e_{u_j^{(p)}} \right).$$

We then compute compatibility scores by viewing the child as a query and the tuple as a key:

$$s_j = \left\langle z_v^{(0)} W_Q, h_{C_j} W_K \right\rangle, \quad C^* \sim \text{Softmax}(s_1, \dots, s_M).$$

**3. Causal Update:** Once the connection is established, the child integrates the chosen parents to form its final latent state:

$$z_v = \text{MLP}_{child} \left( z_v^{(0)} \oplus h_{C^*} \right).$$

Optionally, we apply a feedback update to the chosen parents to control the resulting topology:

$$e_u \leftarrow \text{MLP}_{fb}(e_u \oplus z_v), \quad \forall u \in C^*.$$

This feedback mechanism smoothly interpolates between uniform random attachment (frozen or delayed updates) and preferential attachment (immediate positive updates), enabling diverse degree distributions across generated schemas.

### 5.1.3. STAGE 3: CONTENT COMPLETION

The final stage generates the observable data columns  $\mathcal{D}_{cols}$ . By delaying feature synthesis until the topology is fixed, we ensure that every generated data point is conditioned on the complete, globally-refined structural context.

To approximate the conditional distribution  $P(\mathcal{D}_{cols} | G_{in}, \mathcal{Z})$ , we employ a **Bidirectional Graph Neural Network**. This architecture acts as the practical instantiation of the Hierarchical SCM, propagates the latent causal states across the instance graph to induce correlations.

**1. Relational Message Passing.** We initialize each row-node with its latent state  $h_v^{(0)} = z_v$  and perform  $K$  rounds of heterogeneous propagation on the instance graph. Let  $\tau$  denote a relation type induced by an FK (and  $\tau^{-1}$  its reverse), with neighbor sets  $\mathcal{N}_\tau(v)$  and incident relations  $\mathcal{R}(v)$  as defined in Definition 3.4. We aggregate messages separately per relation type:

$$h_v^{(\ell+1)} = \text{Update} \left( h_v^{(\ell)}, \bigoplus_{\tau \in \mathcal{R}(v)} \underbrace{\sum_{u \in \mathcal{N}_\tau(v)} \text{MLP}_\tau(h_u^{(\ell)})}_{\text{Permutation-invariant over neighbors}} \right)$$

**2. Universal Decoding.** After  $K$  layers, the final embedding  $h_v^{(K)}$  contains a globally contextualized representation

of the row. A shared decoder maps this state to the values of the columns:  $\{A_v\} = \text{MLP}_{dec}(h_v^{(K)})$ . Continuous values are generated via Gaussian heads, while categorical values are sampled via Softmax distributions, completing the synthetic database  $\mathcal{D}$ .

## 5.2. Architectural Implementation

Our backbone is a Transformer adapted for relational data. To bridge the gap between graph-structured RDBs and vector-based architectures, we employ a two-stage process:

**1. Graph Linearization (DFS).** Given a database instance  $\mathcal{D}$  and a target table  $T_*$ , we apply Deep Feature Synthesis (DFS) (Kanter & Veeramachaneni, 2015) as a deterministic linearization operator:  $X = \text{DFS}(\mathcal{D}, T_*) \in \mathbb{R}^{|\mathcal{V}(T_*)| \times p}$ . DFS recursively aggregates relational neighborhoods via (i) *Forward Inheritance* (propagating parent attributes to children) and (ii) *Backward Aggregation* (summarizing child sets with permutation-invariant statistics), yielding a context-enriched single-table representation.

**2. Bi-Attention Reasoning.** We process this linearized input using a simplified TabPFN architecture (Hollmann et al., 2022; Pfefferle et al., 2025). The model alternates between two attention mechanisms to approximate the posterior:

- **Schema Attention (Column-wise):** Attends across features to model inter-feature dependencies. Since DFS features are organized by relational primitives (e.g., aggregations from specific parent/child tables), this attention captures relational signals expressed in the linearized representation.
- **Instance Attention (Row-wise):** Attends across rows to perform In-Context Learning, enabling the query row to leverage patterns from labeled context rows with similar DFS-induced structural summaries.

In this initial release, we employ a binary classification head, as it covers the majority of high-value industrial tasks (e.g., Churn, Fraud). Extensions to multi-class and regression are reserved for future work.

## 5.3. Pretraining Protocol

We adopt a Two-Stage Curriculum to decouple statistical learning from topological reasoning:

- **Stage 1: Tabular Warm-up.** The model is pre-trained on synthetic single-table datasets. This establishes a “statistical backbone,” allowing the model to master distribution matching and outlier detection without structural noise.
- **Stage 2: Relational Adaptation.** We transition to full RDBs generated by our prior. With a stable statistical foundation, the model focuses on interpreting the complex, aggregated signals from DFS, effectively learning to treat topological context as a predictive feature.

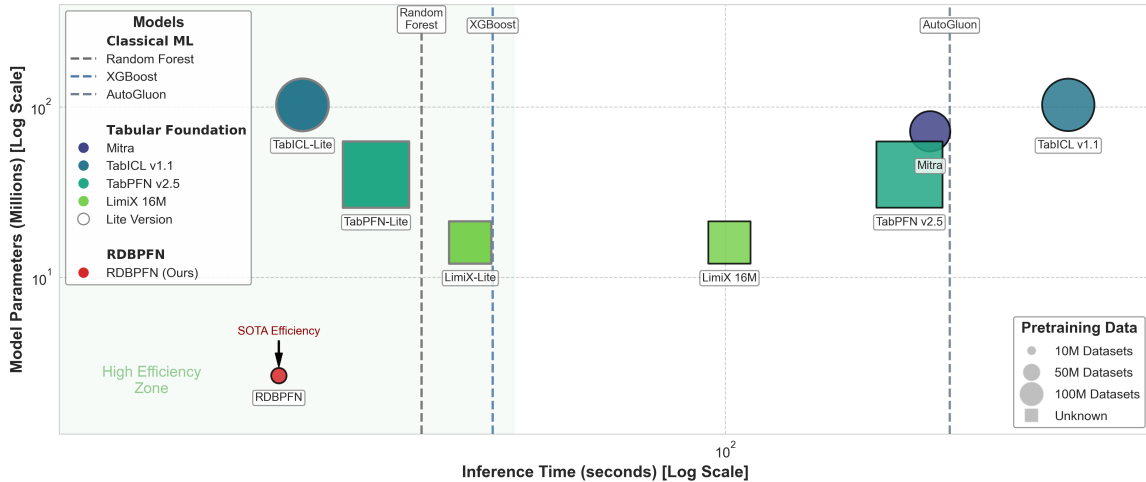


**Figure 2. Resource Efficiency Frontier.** Comparison of model complexity across **Inference Latency** (X-axis), **Parameter Count** (Y-axis), and **Pre-training Data Volume** (Bubble Size). Note that “Lite” baselines denote single-estimator configurations (ensembling disabled) to facilitate a direct architectural comparison. RDB-PFN (red star) dominates the efficiency landscape, achieving SOTA performance with **3x–8x faster** inference, requiring only **2%–5%** of the pre-training data, and utilizing less than **2% to 20%** of the parameters compared to competing foundation models.

## 6. Experiments

We designed our experiments to rigorously evaluate the RDB-PFN as a Foundation Model for relational databases. We structure our analysis around three core questions:

- **RQ1 (RDB Foundation Model Capabilities):** Can RDB-PFN generalize to unseen real-world RDBs without fine-tuning? How does its computational efficiency and architectural complexity compare to existing tabular foundation models?
- **RQ2 (Single-Table Impact):** How does relational pre-training impact performance on standard single-table tasks? Does the model retain general tabular reasoning capabilities despite its specialized prior?
- **RQ3 (Linearized Relational Prior Analysis):** When RDBs are linearized via DFS, what distinguishes their statistical structure from standard single-tabular data?

### 6.1. Experimental Setup

**Datasets.** We evaluate relational reasoning on 19 diverse tasks curated from the 4DBInfer (Wang et al., 2024) and RelBench (Robinson et al., 2024) benchmarks. These tasks span domains including e-commerce, clinical trials, and sports analytics, varying in complexity from simple attribute prediction to complex behavioral modeling requiring temporal aggregation. Extensive prior work has established that these tasks benefit significantly from structure-aware modeling, making them a rigorous testbed for our framework. Additionally, we evaluate single-table performance using a Tabular Benchmark (Grinsztajn et al., 2022). Full dataset statistics are provided in Appendix A.

**Evaluation Protocol.** For the RDB benchmark, we evaluate the aggregated performance across a spectrum of few-shot

context sizes  $N \in \{64, \dots, 1024\}$ . For the single-table benchmark, we downsample each dataset to a maximum of  $N = 1000$  samples. To ensure statistical robustness, we report the mean performance across 10 distinct random seeds for all tasks.

**Baselines.** To benchmark RDB-PFN as a genuine foundation model, we compare against two types of methods:

- **Single-Table Foundation Models (w/ DFS):** We benchmark against state-of-the-art ICL tabular models, including TabPFNv2.5 (Grinsztajn et al., 2025), TablCLv1.1 (Qu et al., 2025), Mitra (Zhang et al., 2025a), and LimiX16M (Zhang et al., 2025b). Because these architectures cannot natively process relational schemas, we provide them with the exact same linearized DFS features used by RDB-PFN to ensure a strictly fair comparison of modeling capabilities. To facilitate direct architectural comparisons, we evaluate both their standard (ensemble) configurations and their “Lite” (single-estimator) variants.
- **Classical Supervised Learning:** We provide reference points using Random Forest (Breiman, 2001), XGBoost (Chen, 2016), and AutoGluon (Erickson et al., 2020). While these methods require iterative fitting (violating the zero-shot ICL constraint), they remain robust industrial baselines. Because raw library defaults often underfit and perform poorly on DFS-generated relational features, we apply lightweight, budgeted hyperparameter optimization to these baselines to ensure they remain competitive without exceeding practical runtime limits.

Detailed configurations and additional analyses of graph-based RDB models are provided in Appendix B.

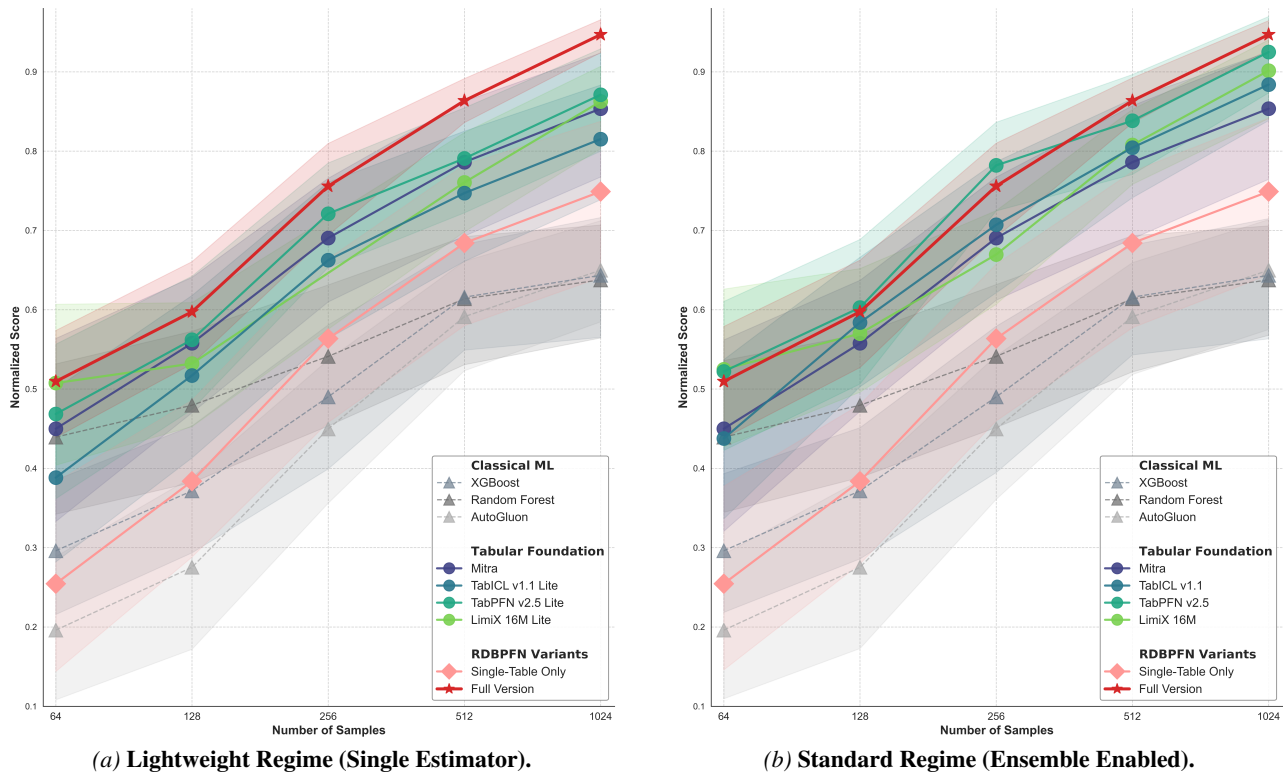


**Figure 3. Relational Few-Shot Performance across Evaluation Protocols.** We report aggregated normalized performance across 19 relational tasks (higher is better). **(a) Single-Estimator Protocol:** all baselines are constrained to one estimator (ensembling disabled). RDB-PFN clearly surpass all baselines. **(b) Recommended-Default Protocol:** baselines run with their official default inference pipelines (which may include test-time ensembling), while RDB-PFN remains a single forward-pass estimator. RDB-PFN maintains superior average performance while offering **3x – 8x faster** inference, positioning it on the optimal frontier of the efficiency-accuracy trade-off.

## 6.2. RQ1: RDB Foundation Model Capabilities

We first establish the performance and computational profile of RDB-PFN on the 19 real-world relational tasks.

**Efficiency & Complexity Analysis.** As illustrated in Figure 2, our framework achieves a highly favorable trade-off between modeling capacity and resource intensity, particularly when considering the hidden inference costs associated with ensembling.

- **Parameter Efficiency:** RDB-PFN utilizes an ultra-compact architecture of only **2.6M parameters**. In contrast, competing single-table foundation models often exceed 100M parameters per estimator.
- **Inference Latency:** RDB-PFN achieves approximately **3x – 8x faster** inference than the default configurations of other tabular foundation models. Even when comparing against “lightweight” baselines (where ensembling is disabled), RDB-PFN maintains superior inference speeds.
- **Data Efficiency:** RDB-PFN is pretrained on only **2 million** datasets, a fraction of the data typically required by tabular foundation models. While the exact pretraining budgets for some models remain undisclosed, other state-of-the-art models use range from tens to hundreds of millions of datasets (e.g., Mitra uses  $\sim 45M$ , TabICLv1.1

uses  $\sim 80M$ , and TabPFNV2 uses  $\sim 130M$ ). Achieving competitive performance with such a constrained data budget validates that our **Relational Prior** serves as a highly effective inductive bias.

**SOTA RDB Few-Shot Performance.** Figure 3 presents the aggregated performance across the benchmark suite.

- **Single-Model Dominance:** When restricted to a strict single-estimator setting (no ensembling), RDB-PFN explicitly outperforms all single-table baselines. This confirms that our Relational Prior yields a superior inductive bias for structural data compared to generic tabular priors.
- **The Efficiency-Performance Frontier:** While baselines can artificially boost performance through computationally expensive ensembling, RDB-PFN still achieves the highest overall average performance using only a single estimator. It delivers superior predictive accuracy while maintaining the rapid inference speed of a lightweight model.

## 6.3. RQ2: Single-Table Performance

To understand the trade-offs of our specialized design, we evaluated RDB-PFN on standard single-table benchmarks (Grinsztajn et al., 2022).

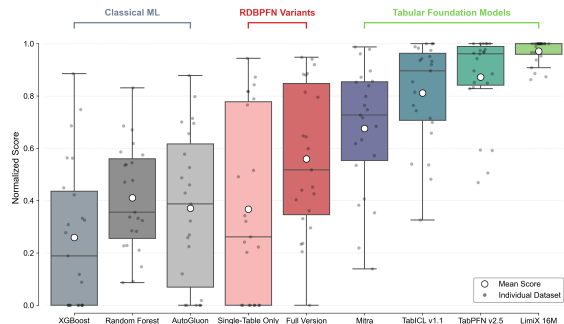


**Figure 4. Single-Table Performance Analysis.** We compare performance across (1) *Classic ML Baselines*, (2) *Specialized Tabular Foundation Models*, and (3) *RDB-PFN Variants*. While RDB-PFN slightly trails specialized single-table models (an expected trade-off given its broader structural scope), it consistently outperforms classical baselines. Crucially, the full RDB-PFN surpasses its own single-table-only variant. This confirms a distinct **Positive Transfer** effect: exposure to diverse relational structures enhances general tabular reasoning capabilities beyond what is achievable with single-table pretraining alone.

**Reasonable Generalization.** As shown in Figure 4, RDB-PFN performs reasonably well, consistently outperforming traditional methods (e.g., XGBoost, Random Forest) in the few-shot regime. Notably, we observe that additional training on RDBs improves performance over our own single-table baseline variant. This suggests that linearized RDBs serve as a diverse data distribution that does not overfit the model to relational data, but rather induces a **positive transfer** that enhances general tabular reasoning.

**The “Specialization Gap”.** RDB-PFN does fall slightly behind specialized single-table foundation models. This result is expected and serves as an important negative control: our model utilizes a vastly simplified single-table pre-training and possesses significantly fewer parameters. This performance gap confirms that our superior results in RQ1 are driven specifically by the learned **Relational Prior**.

#### 6.4. RQ3: Analysis of the Linearized Relational Prior

We hypothesize that RDB-PFN outperforms single-table baselines because it captures a distinct topological signature inherent to relational data. For instance, the DFS process creates clusters of highly correlated columns (e.g., the `Sum` and `Mean` aggregations of the same parent table), which manifest as distinct statistical patterns that standard tabular priors fail to anticipate.

**Visualization Analysis.** Figure 5 compares the correlation matrices of representative datasets. Both real and synthetic single-table datasets exhibit diffuse, unstructured correlation patterns. Conversely, both real and synthetic RDBs display a prominent **Block-Diagonal Structure**, where dense blocks correspond to correlated feature families derived from parent relations. This visual alignment strongly suggests that our synthetic generator effectively models the structural manifold of real-world relational data, allowing the network

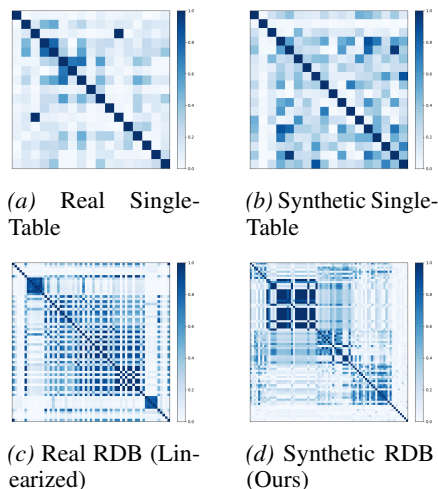


**Figure 5. Visualizing Structural Correlations.** Correlation heatmaps showing that while single-table data (Top Row) exhibits diffuse patterns, linearized RDBs (Bottom Row) display a distinct **Block-Diagonal Structure**. Our synthetic prior successfully reproduces this characteristic real-world topology.

to internalize these dependencies during pretraining.

## 7. Conclusion

We presented RDB-PFN, the first foundation model for RDBs trained entirely on synthetic data. By replacing the standard i.i.d. assumption with a Universal Relational Prior, we developed a framework that enables a single Transformer to perform robust In-Context Learning. Despite using only synthetic data, RDB-PFN outperforms powerful tabular foundation models in both accuracy and efficiency.

## Acknowledgements

This work is supported by the National Key R&D Program of China (2022ZD0160300) and National Natural Science Foundation of China (62276003).

## Impact Statement

This paper presents work whose goal is to advance the field of Machine Learning. There are many potential societal consequences of our work, none which we feel must be specifically highlighted here.

## References

- Achiam, J., Adler, S., Agarwal, S., Ahmad, L., Akkaya, I., Aleman, F. L., Almeida, D., Altenschmidt, J., Altman, S., Anadkat, S., et al. Gpt-4 technical report. *arXiv preprint arXiv:2303.08774*, 2023.
- Arik, S. Ö. and Pfister, T. Tabnet: Attentive interpretable tabular learning. In *Proceedings of the AAAI conference on artificial intelligence*, volume 35, pp. 6679–6687, 2021.

- Bai, J., Wang, J., Li, Z., Ding, D., Zhang, J., and Gao, J. Atj-net: Auto-table-join network for automatic learning on relational databases. In *Proceedings of the Web Conference 2021*, pp. 1540–1551, 2021.
- Balazadeh, V., Kamkari, H., Thomas, V., Li, B., Ma, J., Cresswell, J. C., and Krishnan, R. G. Causalpfn: Amortized causal effect estimation via in-context learning. *arXiv preprint arXiv:2506.07918*, 2025.
- Breiman, L. Random forests. *Machine learning*, 45(1): 5–32, 2001.
- Brown, T., Mann, B., Ryder, N., Subbiah, M., Kaplan, J. D., Dhariwal, P., Neelakantan, A., Shyam, P., Sastry, G., Askell, A., et al. Language models are few-shot learners. *Advances in neural information processing systems*, 33: 1877–1901, 2020.
- Cappuzzo, R., Papotti, P., and Thirumuruganathan, S. Creating embeddings of heterogeneous relational datasets for data integration tasks. In *Proceedings of the 2020 ACM SIGMOD international conference on management of data*, pp. 1335–1349, 2020.
- Chen, T. Xgboost: A scalable tree boosting system. *Cornell University*, 2016.
- Chen, T., Kanatsoulis, C., and Leskovec, J. Relgnn: Composite message passing for relational deep learning. *arXiv preprint arXiv:2502.06784*, 2025.
- Codd, E. F. A relational model of data for large shared data banks. *Communications of the ACM*, 13(6):377–387, 1970.
- Codd, E. F. Relational database: A practical foundation for productivity. In *ACM Turing award lectures*, pp. 1981–2007.
- Cvetkov-Iliev, A., Allauzen, A., and Varoquaux, G. Relational data embeddings for feature enrichment with background information. *Machine Learning*, 112(2):687–720, 2023.
- Cvitkovic, M. Supervised learning on relational databases with graph neural networks. *arXiv preprint arXiv:2002.02046*, 2020.
- Defazio, A., Yang, X., Mehta, H., Mishchenko, K., Khaled, A., and Cutkosky, A. The road less scheduled. *Advances in Neural Information Processing Systems*, 37: 9974–10007, 2024.
- Dooley, S., Khurana, G. S., Mohapatra, C., Naidu, S. V., and White, C. Forecastpfn: Synthetically-trained zero-shot forecasting. *Advances in Neural Information Processing Systems*, 36:2403–2426, 2023.
- Dosovitskiy, A. An image is worth 16x16 words: Transformers for image recognition at scale. *arXiv preprint arXiv:2010.11929*, 2020.
- Du, L., Gao, F., Chen, X., Jia, R., Wang, J., Zhang, J., Han, S., and Zhang, D. Tabularnet: A neural network architecture for understanding semantic structures of tabular data. In *Proceedings of the 27th ACM SIGKDD Conference on Knowledge Discovery & Data Mining*, pp. 322–331, 2021.
- Dwivedi, V. P., Jaladi, S., Shen, Y., López, F., Kanatsoulis, C. I., Puri, R., Fey, M., and Leskovec, J. Relational graph transformer. *arXiv preprint arXiv:2505.10960*, 2025.
- Eremeev, D., Bazhenov, G., Platonov, O., Babenko, A., and Prokhorenkova, L. Turning tabular foundation models into graph foundation models. *arXiv preprint arXiv:2508.20906*, 2025a.
- Eremeev, D., Platonov, O., Bazhenov, G., Babenko, A., and Prokhorenkova, L. Graphpfn: A prior-data fitted graph foundation model. *arXiv preprint arXiv:2509.21489*, 2025b.
- Erickson, N., Mueller, J., Shirkov, A., Zhang, H., Larroy, P., Li, M., and Smola, A. Autogluon-tabular: Robust and accurate automl for structured data. *arXiv preprint arXiv:2003.06505*, 2020.
- Fey, M., Hu, W., Huang, K., Lenssen, J. E., Ranjan, R., Robinson, J., Ying, R., You, J., and Leskovec, J. Relational deep learning: Graph representation learning on relational databases. *arXiv preprint arXiv:2312.04615*, 2023.
- Fey, M., Hu, W., Huang, K., Lenssen, J. E., Ranjan, R., Robinson, J., Ying, R., You, J., and Leskovec, J. Position: Relational deep learning-graph representation learning on relational databases. In *Forty-first International Conference on Machine Learning*, 2024.
- Gorishniy, Y., Rubachev, I., Khulkov, V., and Babenko, A. Revisiting deep learning models for tabular data. *Advances in Neural Information Processing Systems*, 34: 18932–18943, 2021.
- Gorishniy, Y., Rubachev, I., and Babenko, A. On embeddings for numerical features in tabular deep learning. *Advances in Neural Information Processing Systems*, 35: 24991–25004, 2022.
- Gorishniy, Y., Rubachev, I., Kartashev, N., Shlenskii, D., Kotelnikov, A., and Babenko, A. Tabr: Tabular deep learning meets nearest neighbors in 2023. *arXiv preprint arXiv:2307.14338*, 2023.

- Gorishniy, Y., Kotelnikov, A., and Babenko, A. Tabm: Advancing tabular deep learning with parameter-efficient ensembling. *arXiv preprint arXiv:2410.24210*, 2024.
- Grinsztajn, L., Oyallon, E., and Varoquaux, G. Why do tree-based models still outperform deep learning on typical tabular data? *Advances in neural information processing systems*, 35:507–520, 2022.
- Grinsztajn, L., Flöge, K., Key, O., Birkel, F., Jund, P., Roof, B., Jäger, B., Safaric, D., Alessi, S., Hayler, A., et al. Tabpfn-2.5: Advancing the state of the art in tabular foundation models. *arXiv preprint arXiv:2511.08667*, 2025.
- Grover, A. and Leskovec, J. node2vec: Scalable feature learning for networks. In *Proceedings of the 22nd ACM SIGKDD international conference on Knowledge discovery and data mining*, pp. 855–864, 2016.
- Gueye, M., Attabi, Y., and Dumas, M. Row conditional-tgan for generating synthetic relational databases. In *ICASSP 2023-2023 IEEE International Conference on Acoustics, Speech and Signal Processing (ICASSP)*, pp. 1–5. IEEE, 2023.
- Guo, X., Quan, Y., Zhao, H., Yao, Q., Li, Y., and Tu, W. Tabgnn: Multiplex graph neural network for tabular data prediction. *arXiv preprint arXiv:2108.09127*, 2021.
- Harrington, J. L. *Relational database design and implementation*. Morgan Kaufmann, 2016.
- Hayler, A., Huang, X., Ceylan, I. I., Bronstein, M. M., and Finkelshtein, B. Of graphs and tables: Zero-shot node classification with tabular foundation models. In *New Perspectives in Graph Machine Learning*, 2025.
- Hollmann, N., Müller, S., Eggensperger, K., and Hutter, F. Tabpfn: A transformer that solves small tabular classification problems in a second. *arXiv preprint arXiv:2207.01848*, 2022.
- Hollmann, N., Müller, S., Purucker, L., Krishnakumar, A., Körfer, M., Hoo, S. B., Schirrmester, R. T., and Hutter, F. Accurate predictions on small data with a tabular foundation model. *Nature*, 637(8045):319–326, 2025.
- Holzmüller, D., Grinsztajn, L., and Steinwart, I. Better by default: Strong pre-tuned mlps and boosted trees on tabular data. *Advances in Neural Information Processing Systems*, 37:26577–26658, 2024.
- Hoo, S. B., Müller, S., Salinas, D., and Hutter, F. From tables to time: How tabpfn-v2 outperforms specialized time series forecasting models. *arXiv preprint arXiv:2501.02945*, 2025.
- Hu, W., Yuan, Y., Zhang, Z., Nitta, A., Cao, K., Kocijan, V., Sunil, J., Leskovec, J., and Fey, M. Pytorch frame: A modular framework for multi-modal tabular learning. *arXiv preprint arXiv:2404.00776*, 2024.
- Huang, X., Khetan, A., Cvitkovic, M., and Karnin, Z. Tab-transformer: Tabular data modeling using contextual embeddings. *arXiv preprint arXiv:2012.06678*, 2020.
- Hudovernik, V., Xu, M., Shi, J., Šubelj, L., Ermon, S., Štrumbelj, E., and Leskovec, J. Reldiff: Relational data generative modeling with graph-based diffusion models. *arXiv preprint arXiv:2506.00710*, 2025.
- Kanter, J. M. and Veeramachaneni, K. Deep feature synthesis: Towards automating data science endeavors. In *2015 IEEE international conference on data science and advanced analytics (DSAA)*, pp. 1–10. IEEE, 2015.
- Kaplan, J., McCandlish, S., Henighan, T., Brown, T. B., Chess, B., Child, R., Gray, S., Radford, A., Wu, J., and Amodei, D. Scaling laws for neural language models. *arXiv preprint arXiv:2001.08361*, 2020.
- Ke, G., Meng, Q., Finley, T., Wang, T., Chen, W., Ma, W., Ye, Q., and Liu, T.-Y. Lightgbm: A highly efficient gradient boosting decision tree. *Advances in neural information processing systems*, 30, 2017.
- Ketata, M. A., Lüdke, D., Schwinn, L., and Günemann, S. Joint relational database generation via graph-conditional diffusion models. *arXiv preprint arXiv:2505.16527*, 2025.
- Kim, M. J., Grinsztajn, L., and Varoquaux, G. Carte: pre-training and transfer for tabular learning. *arXiv preprint arXiv:2402.16785*, 2024.
- Li, J., Hui, B., Qu, G., Yang, J., Li, B., Li, B., Wang, B., Qin, B., Geng, R., Huo, N., et al. Can llm already serve as a database interface? a big bench for large-scale database grounded text-to-sqls. *Advances in Neural Information Processing Systems*, 36:42330–42357, 2023.
- Li, M., Shitole, V., Chien, E., Man, C., Wang, Z., Sridharan, S., Zhang, Y., Krishna, T., and Li, P. Layerdag: A layer-wise autoregressive diffusion model for directed acyclic graph generation. *arXiv preprint arXiv:2411.02322*, 2024.
- Loshchilov, I. and Hutter, F. Decoupled weight decay regularization. *arXiv preprint arXiv:1711.05101*, 2017.
- Ma, Y., Frauen, D., Javurek, E., and Feuerriegel, S. Foundation models for causal inference via prior-data fitted networks. *arXiv preprint arXiv:2506.10914*, 2025.

- Müller, S., Hollmann, N., Arango, S. P., Grabocka, J., and Hutter, F. Transformers can do bayesian inference. *arXiv preprint arXiv:2112.10510*, 2021.
- Pang, W., Shafieinejad, M., Liu, L., Hazlewood, S., and He, X. Clavaddpm: Multi-relational data synthesis with cluster-guided diffusion models. *Advances in Neural Information Processing Systems*, 37:83521–83547, 2024.
- Patki, N., Wedge, R., and Veeramachaneni, K. The synthetic data vault. In *2016 IEEE international conference on data science and advanced analytics (DSAA)*, pp. 399–410. IEEE, 2016.
- Pfefferle, A., Hog, J., Purucker, L., and Hutter, F. nanotabpfn: A lightweight and educational reimplementation of tabpfn. *arXiv preprint arXiv:2511.03634*, 2025.
- Prokhorenkova, L., Gusev, G., Vorobev, A., Dorogush, A. V., and Gulin, A. Catboost: unbiased boosting with categorical features. *Advances in neural information processing systems*, 31, 2018.
- Qu, J., Holzmann, D., Varoquaux, G., and Morvan, M. L. Tabicl: A tabular foundation model for in-context learning on large data. *arXiv preprint arXiv:2502.05564*, 2025.
- Ranjan, R., Hudovernik, V., Znidar, M., Kanatsoulis, C., Upendra, R., Mohammadi, M., Meyer, J., Palczewski, T., Guestrin, C., and Leskovec, J. Relational transformer: Toward zero-shot foundation models for relational data. *arXiv preprint arXiv:2510.06377*, 2025.
- Ristoski, P. and Paulheim, H. Rdf2vec: Rdf graph embeddings for data mining. In *The Semantic Web–ISWC 2016: 15th International Semantic Web Conference, Kobe, Japan, October 17–21, 2016, Proceedings, Part I 15*, pp. 498–514. Springer, 2016.
- Robertson, J., Reuter, A., Guo, S., Hollmann, N., Hutter, F., and Schölkopf, B. Do-pfn: In-context learning for causal effect estimation. *arXiv preprint arXiv:2506.06039*, 2025.
- Robinson, J., Ranjan, R., Hu, W., Huang, K., Han, J., Dobles, A., Fey, M., Lenssen, J. E., Yuan, Y., Zhang, Z., et al. Relbench: A benchmark for deep learning on relational databases. *Advances in Neural Information Processing Systems*, 37:21330–21341, 2024.
- Somepalli, G., Goldblum, M., Schwarzschild, A., Bruss, C. B., and Goldstein, T. Saint: Improved neural networks for tabular data via row attention and contrastive pre-training. *arXiv preprint arXiv:2106.01342*, 2021.
- Taga, E. O., Ildiz, M. E., and Oymak, S. Timepfn: Effective multivariate time series forecasting with synthetic data. In *Proceedings of the AAAI Conference on Artificial Intelligence*, volume 39, pp. 20761–20769, 2025.
- Wang, M., Gan, Q., Wipf, D., Zhang, Z., Faloutsos, C., Zhang, W., Zhang, M., Cai, Z., Li, J., Mao, Z., et al. 4dbinfer: A 4d benchmarking toolbox for graph-centric predictive modeling on rdbs. *Advances in Neural Information Processing Systems*, 37:27236–27273, 2024.
- Wang, Y., Wang, X., Gan, Q., Wang, M., Yang, Q., Wipf, D., and Zhang, M. Griffin: Towards a graph-centric relational database foundation model. *arXiv preprint arXiv:2505.05568*, 2025.
- Wang, Z. and Sun, J. Transtab: Learning transferable tabular transformers across tables. *Advances in Neural Information Processing Systems*, 35:2902–2915, 2022.
- Yang, Y., Wang, Y., Liu, G., Wu, L., and Liu, Q. Unitabe: A universal pretraining protocol for tabular foundation model in data science. *arXiv preprint arXiv:2307.09249*, 2023.
- Yarullin, R. and Isaev, S. Numerical embeddings for reasoning over text and tables. 2023.
- Ye, H., Yin, H., Zhan, D., and Chao, W. Revisiting nearest neighbor for tabular data: A deep tabular baseline two decades later. *ICLR*, 2(3):4, 2025.
- You, J., Ma, X., Ding, Y., Kochenderfer, M. J., and Leskovec, J. Handling missing data with graph representation learning. *Advances in Neural Information Processing Systems*, 33:19075–19087, 2020.
- Yu, T., Zhang, R., Yang, K., Yasunaga, M., Wang, D., Li, Z., Ma, J., Li, I., Yao, Q., Roman, S., et al. Spider: A large-scale human-labeled dataset for complex and cross-domain semantic parsing and text-to-sql task. *arXiv preprint arXiv:1809.08887*, 2018.
- Yuan, Y., Zhang, Z., He, X., Nitta, A., Hu, W., Wang, D., Shah, M., Huang, S., Stojanović, B., Krumholz, A., et al. Contextgnn: Beyond two-tower recommendation systems. *arXiv preprint arXiv:2411.19513*, 2024.
- Zhang, H., Gan, Q., Wipf, D., and Zhang, W. Gfs: Graph-based feature synthesis for prediction over relational database. *Proceedings of the VLDB Endowment*. ISSN, 2150:8097, 2023.
- Zhang, X., Maddix, D. C., Yin, J., Erickson, N., Ansari, A. F., Han, B., Zhang, S., Akoglu, L., Faloutsos, C., Mahoney, M. W., et al. Mitra: Mixed synthetic priors for enhancing tabular foundation models. *arXiv preprint arXiv:2510.21204*, 2025a.
- Zhang, X., Ren, G., Yu, H., Yuan, H., Wang, H., Li, J., Wu, J., Mo, L., Mao, L., Hao, M., et al. Limix: Unleashing structured-data modeling capability for generalist intelligence. *arXiv preprint arXiv:2509.03505*, 2025b.

Zhu, B., Shi, X., Erickson, N., Li, M., Karypis, G., and Shoaran, M. Xtab: Cross-table pretraining for tabular transformers. *arXiv preprint arXiv:2305.06090*, 2023.

## A. Dataset Details & Evaluation Protocol

### A.1. Relational Benchmark Statistics (4DBInfer & RelBench)

We utilize a suite of 19 diverse predictive tasks derived from 13 distinct relational databases sourced from **4DBInfer** (Wang et al., 2024) and **RelBench** (Robinson et al., 2024). This collection represents a comprehensive cross-section of real-world industrial scenarios, including e-commerce, social networks, and medical research. The selected benchmarks exhibit significant diversity across three key dimensions:

- **Scale:** The datasets range from small-scale scientific studies (e.g., *Rel-Trial* with  $\sim 5.8$ M rows) to massive industrial logs (e.g., *AVS* with  $\sim 350$ M rows), testing the model’s scalability.
- **Topological Complexity:** The schema complexity varies from simple star schemas (e.g., *Amazon* with 3 tables) to deep, multi-hop snowflake schemas (e.g., *Rel-Trial* with 15 tables and 140 columns).
- **Target Distribution:** The tasks cover various difficulties, including highly imbalanced task types.

Table 1. Statistics of relational database datasets.

Dataset	Tables	Columns	Rows
Amazon	3	15	24,291,489
AVS	3	24	349,967,371
Diginetica	5	28	3,672,396
Outbrain	8	31	4,778,954
Retailrocket	3	11	23,033,676
Stackexchange	7	49	5,399,818
Rel-amazon	3	15	24,291,489
Rel-avito	8	43	20,679,117
Rel-event	5	128	41,328,337
Rel-fl	9	77	97606
Rel-hm	3	37	33,265,846
Rel-stack	7	51	38,109,828
Rel-trial	15	140	5,852,157

Table 2. Statistics of relational database tasks.

Dataset	Task Description	#Train / #Val / #Test
Amazon	User Churn Prediction	1,045,568 / 149,205 / 152,486
AVS	Customer Retention Prediction	109,341 / 24,261 / 26,455
Diginetica	Click-through-rate Prediction	108,570 / 6,262 / 5,058
Outbrain	Click-through-rate Prediction	69,709 / 8,715 / 8,718
RetailRocket	Conversion-rate Prediction	80,008 / 9,995 / 9,997
Stackexchange	User Churn Prediction	142,877 / 88,164 / 105,612
Stackexchange	Post Popularity Prediction	308,698 / 38,587 / 38,588
Rel-amazon	User Churn Prediction	4,732,555 / 409,792 / 351,885
Rel-amazon	Item Churn Prediction	2,559,264 / 177,689 / 166,842
Rel-avito	User Clicks Prediction	59,454 / 21,183 / 47,996
Rel-avito	User Visits Prediction	86,619 / 29,979 / 36,129
Rel-event	User Repeat Prediction	3,842 / 268 / 246
Rel-event	User Ignore Prediction	19,239 / 4,185 / 4,010
Rel-fl	Driver DNF Prediction	11,411 / 566 / 702
Rel-fl	Driver Top3 Prediction	1,353 / 588 / 726
Rel-hm	User Churn Prediction	3,871,410 / 76,556 / 74,575
Rel-stack	User Engagement Prediction	1,360,850 / 85,838 / 88,137
Rel-stack	User Badge Prediction	3,386,276 / 247,398 / 255,360
Rel-trial	Study Outcome Prediction	11,994 / 960 / 825

### A.2. Single-Table Benchmark Details

To verify the backward compatibility of RDB-PFN with standard tabular tasks, we evaluate on a subset of the **Tabular Benchmark** proposed by Grinsztajn et al. (2022). While our primary focus is relational reasoning, this evaluation ensures that our architecture maintains competitive performance on “flat” feature matrices.

We selected 23 diverse classification datasets ranging from small-scale tasks (e.g., *Bioresponse*) to larger industrial logs (e.g., *Higgs*, *Coverttype*). Table 3 details the characteristics of these datasets.

Table 3. Statistics of the Single-Table Classification Datasets used for verification. **(Num)** and **(Cat)** denote two variants of the same dataset: one containing exclusively numerical features and one containing categorical features, respectively.

Dataset	# Samples	# Feats	Dataset	# Samples	# Feats
Bioresponse	3,434	419	Default-Credit (Num)	13,272	20
Diabetes130US	71,090	7	Default-Credit (Cat)	13,272	21
Higgs	940,160	24	Electricity (Num)	38,474	7
MagicTelescope	13,376	10	Electricity (Cat)	38,474	8
MiniBooNE	72,998	50	Eye_Movements (Num)	7,608	20
Albert	58,252	31	Eye_Movements (Cat)	7,608	23
Bank-Marketing	10,578	7	HELOC	10,000	22
California	20,634	8	House_16H	13,488	16
Compas-Two-Years	4,966	11	Jannis	57,580	54
Coverttype (Num)	566,602	10	Pol	10,082	26
Coverttype (Cat)	423,680	54	Road-Safety	111,762	32
Credit	16,714	10			

### A.3. Evaluation Protocol

To ensure statistical rigor, we adhere to a standardized few-shot evaluation protocol across all experiments.

**RDB Few-Shot Evaluation.** For relational tasks, we evaluate the model’s ability to learn in-context across a spectrum of data availability regimes.

- **Context Sizes** ( $N_{shot}$ ): We iterate through context lengths of  $k \in \{64, 128, 256, 512, 1024\}$ .
- **Robustness:** For each task and each  $N_{shot}$ , we perform inference over **10 distinct random seeds**. In each run, the context examples are sampled uniformly at random from the training split. We report the mean and standard deviation of the performance metric across these 10 folds to account for variance in context quality.

**Single-Table Verification.** For the single-table benchmarks, we adopt a lightweight, fixed-budget evaluation protocol.

- **Setup:** We fix the dataset size to  $N = 1000$  samples, downsampling larger datasets as necessary.
- **Repeated Trials:** Using the downsampled datasets, we apply a 70%/30% train-test split. We then train and evaluate the model, repeating this process 10 times to ensure statistical stability.

**Task Standardization & Metrics.** In this work, we focus primarily on Binary Classification, which constitutes the vast majority of high-value industrial relational problems (e.g., Churn, CTR, Fraud).

- **Scope:** Consequently, all selected benchmarks are binary classification tasks. Multi-class targets (if any) can be binarized (e.g., “Top-1 vs. Rest”) to align with the current architecture’s output head.
- **Metric:** We report ROC-AUC as the primary metric. ROC-AUC is threshold-independent and robust to the significant class imbalance observed in tasks like *User Churn*.

## B. Baseline Configurations & Analysis

### B.1. Classical Supervised Learning Baselines

To represent the Industrial Standard, we evaluate three widely-used algorithms. Crucially, to ensure a fair comparison of modeling capacity, all baselines are fed the exact same linearized DFS features as RDB-PFN.

- **AutoGluon** (Erickson et al., 2020): We utilize the “medium\_quality” preset, which balances predictive performance with training efficiency.
- **Random Forest** (Breiman, 2001): We observed that the standard configuration (100 estimators) led to rapid inference but significant underfitting on complex relational features. To provide a stronger baseline while maintaining reasonable speed, we increased the capacity by setting the number of estimators to 500.
- **XGBoost** (Chen, 2016): Similarly, standard configurations often resulted in premature convergence and suboptimal performance on this task. We strengthened this baseline by increasing the number of estimators to 5000, reducing the learning rate to 0.01, and increasing the maximum depth to 12. To mitigate overfitting given this increased capacity, we set both “subsample” and “colsample\_bytree” to 0.8.

### B.2. Single-Table Foundation Model Configurations

All single-table foundation models are evaluated using the same DFS-Linearized inputs. For models that support ensembling, we evaluate both the **Default** (ensemble) configuration and a **Lite** (single-estimator) configuration to facilitate a direct comparison with RDB-PFN’s efficiency.

- **TabPFNv2.5** (Grinsztajn et al., 2025): We use the official “tabpfn-v2.5” checkpoint.
  - *Lite Variant*: We disable the default ensembling mechanism (setting  $N_{ens} = 1$ ).
- **TabICLv1.1** (Qu et al., 2025): We utilize the official default checkpoint.
  - *Lite Variant*: We evaluate the model without its standard ensemble aggregation.
- **Mitra** (Zhang et al., 2025a): We use the checkpoint provided via the AutoGluon integration. Note that the default configuration for Mitra already utilizes a single estimator; therefore, no separate “Lite” variant is required.
- **LimiX16M** (Zhang et al., 2025b): We use the official checkpoint.
  - *Preprocessing Adjustment*: We observed that the default SVD preprocessing caused numerical instability and crashes due to the higher noise variance in linearized RDB features. Consequently, we disable SVD preprocessing for all experiments.
  - *Lite Variant*: We evaluate the model with ensembling disabled.

### B.3. Graph-Based RDB Foundation Models

We also investigated Graph-Based RDB foundation models. Unlike single-table approaches, these models ingest raw relational schemas directly, theoretically offering a higher potential to capture complex structural topologies without the information loss inherent in flattening. However, they currently face significant challenges regarding training complexity and scalability.

We examined two leading methods: **Griffin** (Wang et al., 2025) and **RT** (Ranjan et al., 2025). Both primarily focus on supervised fine-tuning and may incorporate label semantics in ways that diverge from our strict in-context learning protocol.

- **Griffin**: This framework’s few-shot evaluation is limited to a subset of datasets and specific shot counts ( $N \in \{512, 4096\}$ ). Furthermore, its primary focus is on *transfer learning* via fine-tuning on domain-specific corpora, rather than providing a single, universal inference engine. Since Griffin provides four distinct model variants rather than a unified foundation model, a direct comparison is challenging.

*Comparison Strategy*: To approximate a comparison, we adopted an “Ensemble” strategy for Griffin: for each task, we selected the best-performing Griffin checkpoint from its respective domain group. Even against this idealized baseline,

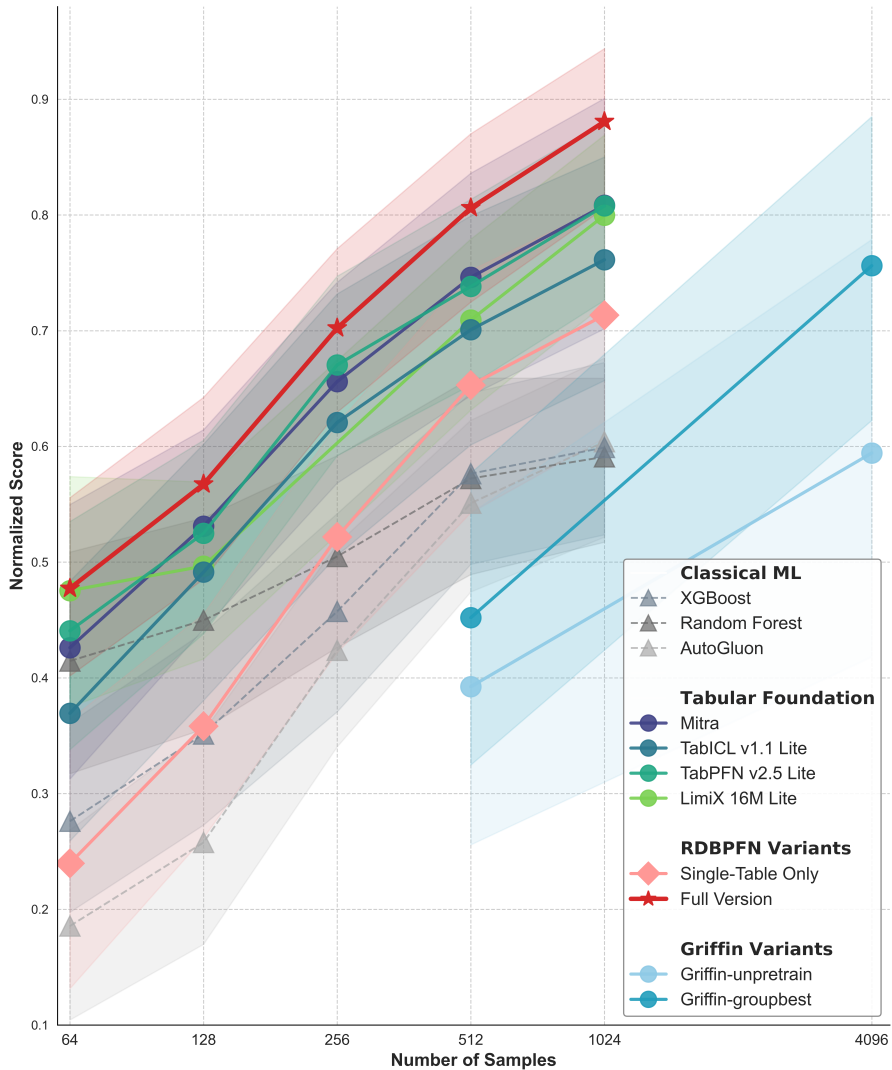


Figure 6. **Comparison with Graph-Based Baselines (Griffin).** We compare RDB-PFN against an idealized “Ensemble” of Griffin on the subset of overlapping tasks. For the baseline, we manually select the best-performing Griffin checkpoint for each specific task group. Despite this advantage, RDB-PFN consistently outperforms Griffin even with less amount of available data, validating that our **Universal Relational Prior** generalizes better than domain-specific fine-tuning.

RDB-PFN consistently achieves superior performance across the intersecting tasks, demonstrating the robustness of our universal prior (shown in figure 6).

- **RT:** While RT explores a zero-shot setting, its methodology differs fundamentally from standard ICL. Although it does not explicitly update model weights using labels, *it injects label information into the database as an auxiliary table during inference*. In their reported results, all labels from the training split were included, allowing the model to potentially leverage significantly more labels than a strict ICL setup. While we acknowledge the value of this approach for certain applications, it constitutes a different experimental paradigm. Consequently, we were unable to establish a strictly fair comparison protocol.

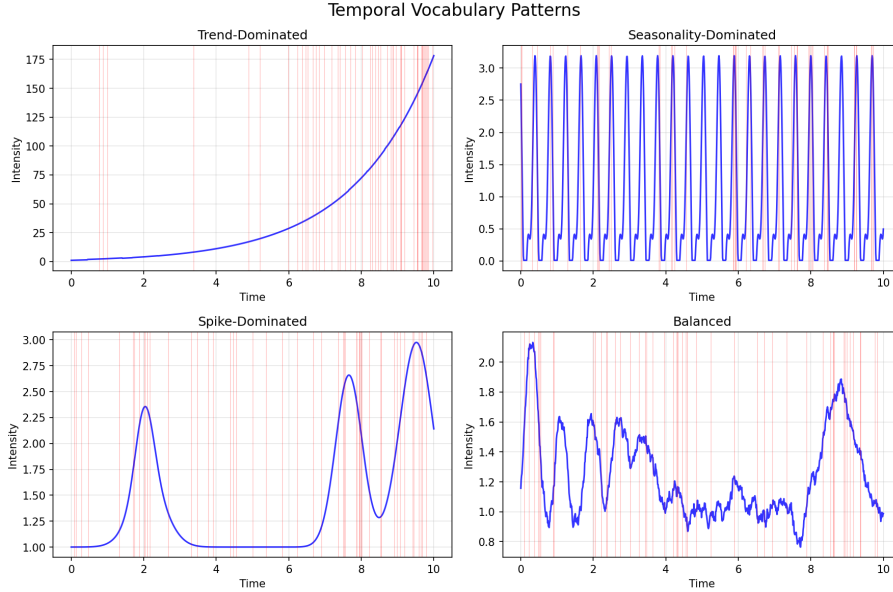


Figure 7. **Diversity of Generated Temporal Patterns.** We visualize the row density over time for four distinct synthetic tables. By composing primitives from our Temporal Vocabulary (Trend, Seasonality, Spike), the prior generates complex, non-i.i.d. distributions.

## C. Implementation Details

### C.1. Data Generation Model Details

#### C.1.1. STAGE 1: SCHEMA GENERATION WITH LAYERDAG

To approximate the complex distribution of realistic database schemas  $P(G_S)$ , we employ LayerDAG (Li et al., 2024), a state-of-the-art autoregressive discrete diffusion model. LayerDAG is uniquely suited for relational schema synthesis because it decomposes DAG generation into a sequence of bipartite layers, a structure that naturally enforces the acyclic dependencies required for valid Foreign Key (FK) joins. The generation process proceeds autoregressively as follows:

- **Layerwise Decomposition:** The model views the schema graph as a topological sequence of layers  $\mathcal{V}^{(1)}, \dots, \mathcal{V}^{(L)}$ . The first layer  $\mathcal{V}^{(1)}$  consists of independent “Source Tables” (root nodes), while subsequent layers contain dependent tables that reference previous layers.
- **Conditional Diffusion:** At each step  $l$ , the model conditions on the partial graph generated so far,  $G^{(\leq l-1)}$ , to generate the next bipartite layer. A discrete diffusion process jointly synthesizes both the table nodes (metadata/attributes) and the FK edges, ensuring that every generated connection respects the logical constraints of the schema.

We pre-train this module on a small corpus of real-world database schemas (Yu et al., 2018; Li et al., 2023). This allows our Relational Prior to sample from a distribution of realistic industrial topologies, ranging from star schemas to deep snowflake structures, which then serve as the structural skeletons for our synthetic data generation.

#### C.1.2. STAGE 2: STRUCTURAL GENERATION DETAILS

The structure generation relies on a selective SCM, where the edge connection probability is also parameterized. The pseudocode detailing the generation of a dependent table is presented in Algorithm 1.

In addition to this, to accurately simulate the diversity of real-world database topologies which range from uniform random graphs to highly skewed scale-free networks, we implement a **Hybrid Sampling Strategy** and a **Temporal Latent Injection** mechanism.

Furthermore, to accurately simulate the diversity of real-world database topologies, which range from uniform random graphs to highly skewed scale-free networks, we implement a **Hybrid Sampling Strategy** and a **Temporal Latent Injection** mechanism.

---

**Algorithm 1** Selective SCM for Foreign-Key Generation (one dependent table)

---

**Require:** Parent row sets  $\{U^{(1)}, \dots, U^{(p)}\}$ , #child rows  $n$ , candidate size  $M$ , params  $\psi$

**Ensure:** FK assignments and latent states  $\{z_v\}$

- 1: **for**  $i = 1$  to  $n$  **do**
  - 2:   Sample child initialization  $z^{(0)} \leftarrow \text{MLP}_{init}(\epsilon)$
  - 3:   Sample candidate parent tuples  $\{C_j\}_{j=1}^M$ , each  $C_j = (u_j^{(1)}, \dots, u_j^{(p)})$
  - 4:   Tuple embed:  $h_{C_j} \leftarrow \text{MLP}_{comb}(e_{u_j^{(1)}} \oplus \dots \oplus e_{u_j^{(p)}})$
  - 5:   Score:  $s_j \leftarrow \langle z^{(0)} W_Q, h_{C_j} W_K \rangle$
  - 6:   Sample  $C^* \sim \text{Softmax}(s_1, \dots, s_M)$  and set FKs accordingly
  - 7:   Update child state:  $z_v \leftarrow \text{MLP}_{child}(z^{(0)} \oplus h_{C^*})$
  - 8:   Optional feedback: for each parent  $u \in C^*$ , update  $e_u \leftarrow \text{MLP}_{fb}(e_u \oplus z_v)$
  - 9: **end for**
- 

**1. Topological Control via Hybrid Sampling.** As posited in the main text, the distribution of node degrees (e.g., the number of Orders associated with a User) can be governed by the parent update frequency. We implement this practically by mixing two distinct generation modes:

- **Mode A: Parallel Generation (Frozen State).** In this mode, we generate child rows without updating parent embeddings at intermediate steps. We sample candidate parent tuples for all child rows in parallel, based on a static snapshot of the parent states. This approximates a uniform random graph process (akin to the Erdős-Rényi model), as high-degree parents do not gain an immediate advantage during batch generation.
- **Mode B: Sequential Generation (Dynamic Feedback).** In this mode, we generate children in small mini-batches. Crucially, after each batch, we execute the causal update step, immediately increasing the selection probability of the chosen parents. This feedback loop enforces **preferential attachment**, leading to long-tailed, scale-free distributions.

By modulating the mixing ratio between Mode A and Mode B, along with the magnitude of the feedback update, we can continuously interpolate between uniform and power-law degree distributions.

**2. Temporal Latent Initialization.** Real-world data is rarely i.i.d.; rather, it exhibits strong temporal dependencies. To capture this, we augment the latent initialization step. Instead of sampling purely from a standard Gaussian distribution, the initial child state  $z^{(0)}$  is conditioned on a **Temporal Vocabulary**:

- **Signal Primitives:** We define a library of three orthogonal temporal signals:
  1. **Trend:** Linear or non-linear drift over time (e.g., a growing user base).
  2. **Seasonality:** Cyclic patterns (e.g., weekly or monthly spending habits).
  3. **Spike:** Sparse, high-magnitude events (e.g., Black Friday sales).
- **Composition:** For each table, we sample a random mixture of these primitives to form a unique temporal signature. This signature modulates the sampling of  $z^{(0)}$ , ensuring that the generated rows reflect diverse temporal evolutions rather than static noise distributions (see Figure 7).

## C.2. Main Model Details

### C.2.1. MODEL ARCHITECTURE

We employ a 6-layer Bidirectional Transformer architecture, optimized for high-throughput inference in resource-constrained environments.

- **Hyperparameters:** The model utilizes an embedding dimension of  $d_{model} = 128$  and 4 parallel attention heads.
- **Efficiency:** This lightweight configuration allows for rapid deployment while retaining sufficient capacity to resolve complex relational patterns via the attention mechanism.

### C.2.2. DFS LINEARIZATION CONFIGURATION

To linearize the relational graph into a sequence compatible with the Transformer, we apply Deep Feature Synthesis (DFS) using a restricted, robust set of aggregation primitives.

- **One-to-Many (Aggregation):** We utilize  $\{\text{Mean, Sum, Max, Min, Count, Mode}\}$  to summarize child records.
- **One-to-One (Transformation):** We employ standard identity mappings to propagate attributes from parent tables directly to child rows.

### C.2.3. TRAINING PROTOCOL

We adopt a Two-Stage Curriculum Learning strategy to stabilize training and progressively introduce relational complexity.

- **Stage 1: Tabular Warm-up (Feature Reasoning).**

The model is initially trained on 600k synthetic *single-table* datasets. This phase focuses on mastering fundamental statistical properties and feature interactions.

- *Data Dimensions:* Fixed context size of 600 rows  $\times$  18 columns.
- *Hardware:* Single NVIDIA RTX 4090 GPU.
- *Optimization:* We use the **Schedule-Free AdamW** optimizer (Defazio et al., 2024; Loshchilov & Hutter, 2017) with a learning rate of  $lr = 5e-4$ .

- **Stage 2: Relational Fine-tuning (Structural Reasoning).**

We continue training on a mixed corpus of approximately 1.8 million synthetic datasets, combining single-table data with complex RDBs generated by our Relational Prior. This phase adapts the model to the structural modality of aggregated features. To efficiently process the expanded corpus and increased structural complexity, training for this stage is distributed across 8 NVIDIA RTX 4090 GPUs.

**1. Dataset Composition.** The training mix is stratified as follows:

- **Single-Table Tasks:**  $\sim 600k$  datasets.
- **Relational Tasks (RDBs):**  $\sim 1.2M$  datasets, comprising:
  - \* Small Prior (1-hop DFS):  $\sim 800k$ .
  - \* Small Prior (2-hop DFS):  $\sim 200k$ .
  - \* Large Prior (1-hop DFS):  $\sim 200k$ .

**2. Feature Standardization (Over-generate & Subsample).**

Since DFS produces feature sets of variable length depending on the schema depth, we employ a standardization strategy to maintain consistent input dimensions. We initially over-compute features by generating 60 columns for 1-hop tasks and 90 columns for 2-hop tasks, and subsequently downsample them to a fixed width of 30 columns. This ensures all Stage 2 tasks share a uniform shape of 600 rows  $\times$  30 columns.

**3. Task Augmentation.**

To maximize data utility, we employ a multi-target sampling strategy. For each generated schema, rather than selecting a single target column, we randomly sample 6 distinct columns to serve as prediction targets. This effectively multiplies the available training instances, forcing the model to reason about different dependency directions within the same structural context.

## D. Proof

**Proof roadmap.** Although the generative pipeline operates chronologically as *Schema*  $\rightarrow$  *Structure*  $\rightarrow$  *Content* (Eq. equation 1), our completeness proof is organized by *lemma dependency* rather than execution order. We first establish the completeness of **Content Completion** (Stage 3), since it reduces to approximating local conditional mechanisms that obey structured, permutation-invariant aggregation over relational neighborhoods. This yields a foundational universality result for our **Hierarchical SCM** architecture. We then leverage this result to prove the completeness of **Structural Generation** (Stage 2), which reuses the same hierarchical aggregation but additionally requires an autoregressive *selection* mechanism to generate foreign-key links (i.e., to route each new child row to appropriate parent rows). Finally, combining the universality of the schema generator (Stage 1) with the completeness of Stages 2–3 gives Theorem D.23.

**From main-text assumptions to proof assumptions.** The main text introduces three principles: schema acyclicity (A4.1), relational Markovian locality (A4.2), and conditional exchangeability (A4.3). The appendix instantiates them as follows:

- **Acyclicity**  $\Rightarrow$  **explicit generation order.** A4.1 implies that tables can be generated in a topological order, formalized as AD.17 for Stage 2.
- **Locality**  $\Rightarrow$  **bounded-hop parent sets.** A4.2 becomes (i) cell-level local parent sets for content generation (AD.9, Stage 3) and (ii) row-level local dependence for structural link/latent generation (AD.18, Stage 2).
- **Exchangeability**  $\Rightarrow$  **shared, permutation-invariant mechanisms.** A4.3 is realized as mechanism sharing by feature type and hierarchy-respecting, permutation-invariant aggregation (AD.11–AD.12, Stage 3) and by table/relation-level sharing for structure generation (AD.19, Stage 2).

In addition, the appendix introduces a small number of technical conditions that are not meant as new domain claims but as *operational regularity assumptions* enabling a tractable hierarchical factorization (e.g., feature-type ordering AD.7 and typewise conditional independence AD.8; deterministic PK encoding AD.16). These conditions specify *how* the high-level principles are realized in our modular generators.

### D.1. Preliminaries

We adopt the schema/instance notation and graph constructions from Section 3, in particular Definitions 3.1–3.3. Note that in Section 3 we used  $v \in \mathcal{V}_{in}$  for a row-node; in the appendix we reserve  $v = (r, c)$  (Definition D.1) for a *cell instance* and use  $r$  for row or row-nodes to avoid clashes.

**Definition D.1** (Cell Instances and Values). For the proofs, we work at the **cell-instance** level. We reserve  $v = (r, c)$  to denote a cell instance, where  $r \in \mathcal{V}(T)$  is a row and  $c \in \mathcal{C}(T)$  is a column of the same table. Let

$$\mathcal{V} := \{(r, c) : T \in \mathcal{T}, r \in \mathcal{V}(T), c \in \mathcal{C}(T)\}$$

be the set of all cell instances in the database instance. We denote the value stored at cell instance  $v = (r, c)$  by the random variable  $A_v$ .

We also use the canonical projection maps:

$$\text{RowOf}(v) = r, \quad \text{ColumnOf}(v) = c, \quad \text{TableOf}(v) = T \text{ where } T \text{ is the unique table such that } r \in \mathcal{V}(T).$$

**Definition D.2** (Structural vs. Dependent Columns and Cell Instances). Fix a schema  $G_S$  and row sets  $\{\mathcal{V}(T)\}_{T \in \mathcal{T}}$ . Let  $\mathcal{V}$  be the set of all cell instances  $v = (r, c)$ .

We define the *structural column types* as key columns plus any additional connectivity-defining columns:

$$\mathcal{C}^{struct} := \left( \bigcup_{T \in \mathcal{T}} \mathcal{K}^{pk}(T) \right) \cup \left( \bigcup_{T \in \mathcal{T}} \mathcal{K}^{fk}(T) \right) \cup \mathcal{C}^{conn},$$

where  $\mathcal{C}^{conn}$  denotes any (optional) non-key columns whose values are used by the structural generator to determine connectivity (and is empty if no such columns are used). And define the corresponding structural cell instances

$$\mathcal{V}^{struct} := \{(r, c) \in \mathcal{V} : c \in \mathcal{C}^{struct}\}.$$

All remaining *feature* columns are *dependent columns*:

$$\mathcal{A}^{dep} := \bigcup_{T \in \mathcal{T}} \mathcal{A}(T), \quad \mathcal{V}^{dep} := \{(r, c) \in \mathcal{V} : c \in \mathcal{A}^{dep}\}.$$

We denote the realized values on structural cells by  $\mathcal{D}_{struct} := \{A_v\}_{v \in \mathcal{V}^{struct}}$  and on dependent cells by  $\mathcal{D}_{dep} := \{A_v\}_{v \in \mathcal{V}^{dep}}$ .

**Definition D.3** (Structural Latent States). In addition to key columns, Stage 2 may generate a latent state  $Z_r \in \mathbb{R}^d$  for each row-node  $r \in \mathcal{V}_{in}$ , representing structural characteristics used for subsequent content generation. We denote the collection of all latent row states by  $\mathcal{Z} := \{Z_r\}_{r \in \mathcal{V}_{in}}$ .

## D.2. Single-Table Completeness

We begin with the foundational case of a single table. Let the database contain only one table  $T$  with columns  $\mathcal{C}(T) = \{c_1, \dots, c_m\}$ . Let  $\mathcal{V}(T)$  denote its (finite) set of rows. For any row  $r \in \mathcal{V}(T)$  and column  $c \in \mathcal{C}(T)$ , the corresponding cell instance is  $v = (r, c)$  and its value is denoted by  $A_v$  (Definition D.1).

To describe the data-generating process, we introduce a *generic row* random vector

$$\mathbf{A} := (A_1, \dots, A_m), \quad \text{where } A_k \text{ represents the value of column } c_k \text{ in a random row.}$$

Thus, a realized row  $r$  corresponds to one sample  $\mathbf{a}_r = (a_{r,1}, \dots, a_{r,m})$  from the joint distribution  $P(\mathbf{A})$ . Equivalently, for each column  $c_k \in \mathcal{C}(T)$  we have  $A_{(r,c_k)} = a_{r,k}$ , and  $A_k$  denotes the random value of column  $c_k$  in a generic row.

**Assumption D.4** (Row i.i.d.). Rows in table  $T$  are independent and identically distributed draws from a fixed row distribution:

$$\mathbf{a}_r \sim_{i.i.d.} P(\mathbf{A}) \quad \text{for all } r \in \mathcal{V}(T).$$

**Justification** Assumption D.4 formalizes the standard single-table modeling view used throughout classical statistics and most tabular learning benchmarks: a table is treated as a multiset of records drawn from a common population distribution. This perspective is also implicit in early tabular foundation model constructions such as prior-data fitted networks (e.g., TabPFNv1, TabICL), where a *dataset-level* generative mechanism is sampled once (e.g., an SCM with parameters  $\theta_{\text{SCM}}$ ), and then individual rows are generated independently by drawing fresh exogenous noise for each row. In this view, the table exhibits a *global mechanism* shared across all rows within the dataset, while randomness arises from per-row noise, making rows exchangeable and (under the simplest setting) i.i.d. We emphasize that this i.i.d. assumption is a *baseline* used to build intuition and establish a clean completeness result. Many real-world tables deviate from i.i.d. sampling due to temporal ordering, distribution shift, repeated measurements, or group-level correlations, and are already attempted to be handled by later work (e.g., TabPFNv2). However, these extensions are orthogonal to the core message here: in the simplest and most widely used single-table setting, an SCM-style shared mechanism with independent per-row noise yields the i.i.d. formulation captured by Assumption D.4.

**Lemma D.5** (Universal measurable conditional sampler + approximation transfer). *Let  $(X, Y)$  be random variables with  $Y$  taking values in a standard Borel space (e.g.,  $\mathbb{R}^d$ , any countable set, any finite set, or a product of these). Then there exists a Borel measurable function  $f$  and an independent  $U \sim \text{Unif}(0, 1)$  such that*

$$Y \stackrel{d}{=} f(X, U).$$

Moreover, if  $\hat{f}_n$  is any sequence of measurable functions such that  $\hat{f}_n(X, U) \rightarrow f(X, U)$  in probability under the joint law of  $(X, U)$ , then

$$\hat{f}_n(X, U) \Rightarrow f(X, U).$$

*Proof sketch.* The first statement is a standard randomization lemma for regular conditional distributions on standard Borel spaces: sample  $Y$  by applying a measurable map to  $(X, U)$ . The second statement follows from the Continuous Mapping Theorem / Slutsky-style arguments on pushforward measures: convergence in probability of the outputs implies weak convergence of the output laws.  $\square$

**Theorem D.6** (Single-Table SCM Completeness). *Fix any joint distribution  $P(A_1, \dots, A_m)$  satisfying Assumption D.4, and fix any ordering  $(A_1, \dots, A_m)$ . Assume each  $A_k$  takes values in a standard Borel space (so that a conditional CDF and generalized inverse are well-defined; e.g., discrete sets or subsets of  $\mathbb{R}$ ). Then there exist measurable functions*

$$f_k : \text{val}(A_{<k}) \times [0, 1] \rightarrow \text{val}(A_k), \quad k = 1, \dots, m,$$

and independent noise variables  $U_k \sim \text{Unif}(0, 1)$  such that the SCM

$$A_k = f_k(A_{<k}, U_k), \quad k = 1, \dots, m,$$

induces exactly the joint distribution  $P(A_1, \dots, A_m)$ .

Moreover, if  $\hat{f}_k$  are chosen from universal approximator classes (for the relevant notion of approximation under the input distribution), then the SCM with  $\hat{f}_k$  can approximate  $P(A_1, \dots, A_m)$  to arbitrary precision in distribution.

*Proof sketch.* Fix an ordering  $(A_1, \dots, A_m)$ . By the chain rule,

$$P(A_1, \dots, A_m) = \prod_{k=1}^m P(A_k \mid A_{<k}).$$

Apply Lemma D.5 to each conditional: for every  $k$  there exists a measurable  $f_k$  and independent  $U_k \sim \text{Unif}(0, 1)$  such that

$$A_k \stackrel{d}{=} f_k(A_{<k}, U_k).$$

Composing these samplers yields an SCM that reproduces the target joint distribution.

For approximation, choose  $\hat{f}_k$  from a universal approximator class so that  $\hat{f}_k(A_{<k}, U_k) \rightarrow f_k(A_{<k}, U_k)$  in probability under the induced input law. Iterating Lemma D.5 (approximation transfer) over  $k = 1, \dots, m$  implies that the induced joint distribution converges to  $P(A_1, \dots, A_m)$ .  $\square$

### D.3. Multi-Table Completeness

We now extend the single-table analysis to a full relational database with multiple tables. Our goal is to characterize and approximate the joint distribution of all cell values in an RDB.

In the single-table setting, the set of variables (columns) is fixed. In the relational setting, however, the set of variables and their allowed link structure depend on the schema. Formally, the schema graph  $G_S$  (Definition 3.3) specifies which tables exist and which foreign-key relations are permitted. Given  $G_S$  and the row sets  $\{\mathcal{V}(T)\}_{T \in \mathcal{T}}$ , the set of cell instances  $\mathcal{V} = \{(r, c) : r \in \mathcal{V}(T), c \in \mathcal{C}(T)\}$  is well-defined (Definition D.1). We therefore consider the conditional joint distribution over all cell values,

$$P(\{A_v\}_{v \in \mathcal{V}} \mid G_S).$$

**Three-stage decomposition.** We instantiate the same *Schema*  $\rightarrow$  *Structure*  $\rightarrow$  *Content* decomposition as in the main text (Eq. equation 1), and adopt consistent stage numbering:

- **Stage 1 (Schema):** sample a schema graph  $G_S$ .
- **Stage 2 (Structure):** generate the *structural skeleton* of the instance, including key columns  $\mathcal{D}_{struct} = \{A_v\}_{v \in \mathcal{V}_{struct}}$  (Definition D.2) and, optionally, latent row states  $\mathcal{Z} = \{Z_r\}_{r \in \mathcal{V}_{in}}$  (Definition D.3). The realized structure induces (or equivalently includes) the instance graph  $G_{in}$ .
- **Stage 3 (Content):** generate all remaining feature values  $\mathcal{D}_{dep} = \{A_v\}_{v \in \mathcal{V}_{dep}}$  conditioned on the realized structure (and  $G_S$ ).

Accordingly, by the chain rule we write the database distribution as

$$P(\mathcal{D}) = \underbrace{P(G_S)}_{\text{Stage 1: Schema}} \cdot \underbrace{P(\mathcal{D}_{struct}, \mathcal{Z} \mid G_S)}_{\text{Stage 2: Structure}} \cdot \underbrace{P(\mathcal{D}_{dep} \mid \mathcal{D}_{struct}, \mathcal{Z}, G_S)}_{\text{Stage 3: Content}}.$$

**Stage 1 (schema) as a modular prior.** We treat  $P(G_S)$  as an external schema prior (hand-designed or learned). Since our focus is on instance generation conditioned on  $G_S$ , we do not further analyze Stage 1 beyond assuming it can represent distributions over finite schema DAGs.

**What remains to prove.** We focus on the completeness of Stage 3 (Content) and Stage 2 (Structure). Following the roadmap stated earlier, we prove Stage 3 first because it reduces to approximating local conditional mechanisms with structured aggregation over relational neighborhoods; we then reuse this result inside the Stage 2 proof, which introduces an additional selection mechanism for generating foreign-key links.

## D.3.1. STAGE 3: CONDITIONAL FEATURE GENERATION (CONTENT COMPLETION)

**Setting.** Fix a schema  $G_S$ . Suppose Stage 2 has generated the structural skeleton  $\mathcal{D}_{struct} = \{A_v\}_{v \in \mathcal{V}^{struct}}$  (Definition D.2) and latent row states  $\mathcal{Z} = \{Z_r\}_{r \in \mathcal{V}_{in}}$  (Definition D.3). Given  $(G_S, \mathcal{D}_{struct})$ , the instance graph  $G_{in}$  is induced by referential integrity (Definition 3.3). Stage 3 models the conditional distribution of all dependent feature values:

$$P(\{A_v\}_{v \in \mathcal{V}^{dep}} \mid \mathcal{D}_{struct}, \mathcal{Z}, G_S).$$

For brevity, let

$$C_2 := (\mathcal{D}_{struct}, \mathcal{Z}, G_S) \quad (\text{equivalently, } C_2 = (G_{in}, \mathcal{Z}, G_S)).$$

We use the dependent feature types  $\mathcal{A}^{dep}$  and dependent cell instances  $\mathcal{V}^{dep}$  as defined in Definition D.2. For each feature type  $a \in \mathcal{A}^{dep}$  define its instance set

$$\mathcal{V}_a^{dep} := \{v \in \mathcal{V}^{dep} : \text{ColumnOf}(v) = a\}.$$

A naive autoregressive factorization over all  $v \in \mathcal{V}^{dep}$  is generally intractable. We therefore introduce a hierarchical factorization based on feature types, with locality defined relative to the fixed instance graph  $G_{in}$  and the structural states  $\mathcal{Z}$ .

**Assumption D.7** (Feature-Type Ordering). There exists a global topological ordering  $\mathcal{O} = (a_1, \dots, a_M)$  of all dependent feature types  $\mathcal{A}^{dep}$ .

**Assumption D.8** (Typewise Conditional Independence). Given  $C_2$  and all dependent features from preceding types  $\{A_u\}_{u \in \mathcal{V}_{<a}^{dep}}$  (where  $a' < a$  denotes precedence in the global order  $\mathcal{O}$ , and  $\mathcal{V}_{<a}^{dep} := \bigcup_{a' < a} \mathcal{V}_{a'}^{dep}$ ), the dependent feature instances of the current type  $a$  are conditionally independent:

$$P(\{A_v\}_{v \in \mathcal{V}_a^{dep}} \mid C_2, \{A_u\}_{u \in \mathcal{V}_{<a}^{dep}}) = \prod_{v \in \mathcal{V}_a^{dep}} P(A_v \mid C_2, \{A_u\}_{u \in \mathcal{V}_{<a}^{dep}}).$$

**Assumption D.9** (Structured Local Dependency). For each dependent cell instance  $v \in \mathcal{V}^{dep}$ , there exists a parent set  $Pa(v) \subseteq \mathcal{V}^{struct} \cup \mathcal{V}_{<\text{ColumnOf}(v)}^{dep}$  such that

$$P(A_v \mid C_2, \{A_u\}_{u \in \mathcal{V}_{<\text{ColumnOf}(v)}^{dep}}) = P(A_v \mid \{A_u\}_{u \in Pa(v)}, Z_{\text{RowOf}(v)}).$$

Moreover,  $Pa(v)$  is relationally local: every  $u \in Pa(v)$  lies either in the same row as  $v$  or in a row within  $k$  hops of  $\text{RowOf}(v)$  in  $G_{in}$  (for a fixed constant  $k$ ). Here  $\mathcal{V}_{<\text{ColumnOf}(v)}^{dep}$  denotes the union of dependent cell instances whose *feature types* precede  $\text{ColumnOf}(v)$  in the global order  $\mathcal{O}$ .

**Corollary D.10** (Hierarchical Factorization for Stage 3). Under Assumptions D.7–D.9, the Stage 3 conditional distribution factorizes as

$$P(\{A_v\}_{v \in \mathcal{V}^{dep}} \mid C_2) = \prod_{a \in \mathcal{O}} \prod_{v \in \mathcal{V}_a^{dep}} P(A_v \mid \{A_u\}_{u \in Pa(v)}, Z_{\text{RowOf}(v)}).$$

*Proof.* By the chain rule applied over the feature-type order  $\mathcal{O}$  (Assumption D.7),

$$P(\{A_v\}_{v \in \mathcal{V}^{dep}} \mid C_2) = \prod_{a \in \mathcal{O}} P(\{A_v\}_{v \in \mathcal{V}_a^{dep}} \mid C_2, \{A_u\}_{u \in \mathcal{V}_{<a}^{dep}}).$$

By typewise conditional independence (Assumption D.8),

$$P(\{A_v\}_{v \in \mathcal{V}_a^{dep}} \mid C_2, \{A_u\}_{u \in \mathcal{V}_{<a}^{dep}}) = \prod_{v \in \mathcal{V}_a^{dep}} P(A_v \mid C_2, \{A_u\}_{u \in \mathcal{V}_{<a}^{dep}}).$$

Finally, by structured local dependency (Assumption D.9), for each  $v \in \mathcal{V}_a^{dep}$  we have

$$P(A_v \mid C_2, \{A_u\}_{u \in \mathcal{V}_{<a}^{dep}}) = P(A_v \mid \{A_u\}_{u \in Pa(v)}, Z_{\text{RowOf}(v)}),$$

which yields the stated factorization.  $\square$

**Assumption D.11** (Mechanism Sharing by Type). All dependent feature instances of the same type share an identical conditional mechanism. That is, for each  $a \in \mathcal{A}^{dep}$ , there exists a conditional distribution  $K_a$  such that

$$P(A_v \mid \{A_u\}_{u \in Pa(v)}, Z_{\text{RowOf}(v)}) = K_a(A_v \mid \{A_u\}_{u \in Pa(v)}, Z_{\text{RowOf}(v)}) \quad \forall v \in \mathcal{V}_a^{dep}.$$

**Assumption D.12** (Hierarchical Parent Processing). The mechanism  $K_a$  must process the parent set  $Pa(v)$  in a way that respects the RDB hierarchy. Let  $R_v := \{\text{RowOf}(u) : u \in Pa(v)\}$  be the set of unique parent rows and  $T_v := \{\text{TableOf}(u) : u \in Pa(v)\}$  the set of unique parent tables.

- **(a) Intra-row coherence (ordered)**. For each parent row  $r \in R_v$ , the parent cells from that row,  $\{u \in Pa(v) : \text{RowOf}(u) = r\}$ , must be processed in a fixed canonical order. The row latent  $Z_r$  may be injected as an additional “row token” in this ordered processing.
- **(b) Inter-row invariance (unordered)**. Within each parent table  $T \in T_v$ , the mechanism must be permutation-invariant to the order of row-level representations coming from rows  $r \in \mathcal{V}(T) \cap R_v$ .
- **(c) Inter-table coherence (ordered)**. The mechanism must process the table-level representations for tables in  $T_v$  in a fixed canonical order (e.g., a fixed schema order or a topological order induced by  $G_S$ ).

**Corollary D.13** (Hierarchical SCM Architecture with Latents). *Under Assumptions D.11 and D.12, each mechanism  $K_a$  can be realized by an SCM  $f_a$  that computes  $A_v$  via bottom-up hierarchical aggregation over  $Pa(v)$ , with row-latent injection:*

$$A_v = f_a(Pa(v), Z_{\text{RowOf}(v)}, U_v) = f'_a(z_v, U_v), \quad (2)$$

$$z_r = h^{\text{row}}(\text{Concat}(Z_r, [A_u : u \in Pa(v), \text{RowOf}(u) = r])), \quad (3)$$

$$z_T = \text{Agg}^{\text{table}}(\{z_r : r \in R_v, r \in \mathcal{V}(T)\}), \quad (4)$$

$$z_v = h^{\text{global}}(\text{Concat}(\{z_T : T \in T_v\}, Z_{\text{RowOf}(v)})). \quad (5)$$

Here  $h^{\text{row}}$  and  $h^{\text{global}}$  are order-sensitive functions (e.g., MLPs over concatenations), and  $\text{Agg}^{\text{table}}$  is permutation-invariant (e.g., Deep Sets).

*Proof.* This is constructive. Eq. equation 3 enforces ordered intra-row processing (AD.12a) and allows injecting the row latent  $Z_r$  as additional row-level context. Eq. equation 4 aggregates row representations within each table in a permutation-invariant manner (AD.12b). Eq. equation 5 processes table representations in canonical order (AD.12c) and can additionally condition on the target row latent  $Z_{\text{RowOf}(v)}$ .  $\square$

**Theorem D.14** (Completeness of Stage 3 (Content Completion)). *Let  $P(\{A_v\}_{v \in \mathcal{V}^{dep}} \mid C_2)$  satisfy Assumptions D.7–D.12. Then there exist hierarchical SCMs  $\{\hat{f}_a\}_{a \in \mathcal{A}^{dep}}$  of the form in Corollary D.13 and independent noises  $U_v \sim \text{Unif}(0, 1)$  such that*

$$A_v = \hat{f}_{\text{ColumnOf}(v)}(Pa(v), Z_{\text{RowOf}(v)}, U_v), \quad v \in \mathcal{V}^{dep},$$

*approximates  $P(\{A_v\}_{v \in \mathcal{V}^{dep}} \mid C_2)$  arbitrarily well in distribution.*

*Proof. Step 1 (Reduction to local mechanisms).* By Corollary D.10, it suffices to approximate each local conditional kernel

$$K_a(A_v \mid \{A_u\}_{u \in Pa(v)}, Z_{\text{RowOf}(v)}) \quad (v \in \mathcal{V}_a^{dep}).$$

**Step 2 (Sampling representation + approximation transfer).** Fix a type  $a$  and a cell instance  $v \in \mathcal{V}_a^{dep}$ . Let

$$X_v := \left( \{A_u\}_{u \in Pa(v)}, Z_{\text{RowOf}(v)} \right), \quad Y_v := A_v.$$

By Lemma D.5, there exists a measurable sampler  $f_a$  and an independent  $U_v \sim \text{Unif}(0, 1)$  such that

$$A_v \stackrel{d}{=} f_a(X_v, U_v).$$

Moreover, if  $\hat{f}_a(X_v, U_v) \rightarrow f_a(X_v, U_v)$  in probability under the induced input law of  $X_v$ , then  $\hat{f}_a(X_v, U_v) \Rightarrow f_a(X_v, U_v)$ .

**Step 3 (Existence of  $\hat{f}_a$  within the hierarchical SCM class).** Assumptions D.11–D.12 restrict  $f_a$  to be *hierarchy-respecting* in its dependence on  $Pa(v)$ : ordered within each parent row, permutation-invariant over parent rows within a table, and ordered across tables. The architecture in Corollary D.13 is universal for this function class because: (i)  $h^{\text{row}}$  and  $h^{\text{global}}$  are chosen from universal approximator classes for order-sensitive maps, and (ii)  $\text{Agg}^{\text{table}}$  is chosen from a universal permutation-invariant set-function class. Therefore, there exists a sequence  $\hat{f}_a$  in this architecture such that  $\hat{f}_a(X_v, U_v) \rightarrow f_a(X_v, U_v)$  in probability under the induced input law.

**Step 4 (Joint convergence of Stage 3).** Approximating each factor in the product of Corollary D.10 and using independence of  $\{U_v\}$  yields convergence of the induced joint Stage 3 conditional distribution.  $\square$

**Connection to the practical GNN decoder.** The Stage 3 proof is stated in terms of a hierarchy-respecting conditional mechanism  $K_a$ . In the main model, we implement this mechanism by a bidirectional relational GNN over  $G_{in}$  with a shared decoder. This choice is compatible with the proof: message-passing layers compute permutation-equivariant summaries of  $k$ -hop neighborhoods, and the decoder realizes the final conditional sampling step.

**Proposition D.15** (GNN as an instantiation of Stage 3 mechanisms). *For any fixed hop radius  $k$ , a  $k$ -layer relational message passing network with permutation-invariant aggregation can approximate the bounded-hop, permutation-equivariant neighborhood summaries required by Corollary D.13, under standard expressivity conditions on the per-relation MLPs and an injective set aggregator.*

*Proof sketch.* Both constructions compute row-wise representations by composing (i) order-sensitive intra-row processing and (ii) permutation-invariant aggregation across sets of neighbors, repeated over a bounded-hop neighborhood. Universal approximation of the constituent MLPs yields approximation of the resulting neighborhood-to-representation map, and the decoder then approximates the conditional output distribution using standard inverse-transform/categorical sampling.  $\square$

### D.3.2. STAGE 2: STRUCTURAL GENERATION (KEYS, LINKS, AND LATENT STATES)

**Setting.** Fix a schema  $G_S$ . Stage 2 models  $P(\mathcal{D}_{struct}, \mathcal{Z} \mid G_S)$ , where  $\mathcal{D}_{struct}$  are structural cells (Definition D.2) and  $\mathcal{Z} = \{Z_r\}_{r \in \mathcal{V}_{in}}$  are optional row latents (Definition D.3). For convenience we denote the key-cell subsets

$$\mathcal{V}^{pk} := \{(r, c) \in \mathcal{V} : c \in \bigcup_{T \in \mathcal{T}} \mathcal{K}^{pk}(T)\}, \quad \mathcal{V}^{fk} := \{(r, c) \in \mathcal{V} : c \in \bigcup_{T \in \mathcal{T}} \mathcal{K}^{fk}(T)\}, \quad \mathcal{V}^{conn} := \{(r, c) \in \mathcal{V} : c \in \mathcal{C}^{conn}\},$$

so that  $\mathcal{V}^{struct} = \mathcal{V}^{pk} \cup \mathcal{V}^{fk} \cup \mathcal{V}^{conn}$ . To keep notation light, the completeness argument below is written for the common case  $\mathcal{C}^{conn} = \emptyset$  (i.e.,  $\mathcal{V}^{conn} = \emptyset$ ); the extension to  $\mathcal{C}^{conn} \neq \emptyset$  follows by including  $\mathcal{V}^{conn}$  among the generated structural cells and in the structural context  $\text{Ctx}(\cdot)$  defined below.

Stage 3 conditions on a fixed realized structure and models feature values via local parent sets  $Pa(v)$  at the cell level. Stage 2, in contrast, must model the *structure itself* (FK links), which naturally introduces (i) a schema-respecting generation order (to satisfy referential integrity) and (ii) possible *competition/degree effects* among parent rows. Accordingly, Stage 2 mirrors Stage 3’s five-assumption style (ordering, locality, sharing, structured processing), but replaces Stage 3’s within-type conditional independence with a restricted dependence on a permutation-invariant competition summary.

**Assumption D.16** (Deterministic Primary Keys). For each table  $T$  with  $n_T := |\mathcal{V}(T)|$  rows, primary key values are a deterministic, known injective encoding of row identity. Concretely, there exists a known injective map  $\text{PKENC}_T : \{1, \dots, n_T\} \rightarrow \text{val}(\mathcal{K}^{pk}(T))$  such that the PK cells of the  $i$ -th row equal  $\text{PKENC}_T(i)$ . Hence PK values carry no causal/content information beyond identifying rows.

Under Assumption D.16, Stage 2 reduces to modeling the joint distribution of (i) all foreign-key cells (equivalently, the induced instance graph  $G_{in}$ ), and (ii) the latent row states  $\mathcal{Z}$ :

$$P(\mathcal{D}_{struct}, \mathcal{Z} \mid G_S) = P(\{A_v\}_{v \in \mathcal{V}^{fk}}, \mathcal{Z} \mid G_S), \quad \text{with } G_{in} = g(G_S, \mathcal{D}_{struct}).$$

For each dependent table  $T$ , fix a row order  $\pi_T = (r_{T,1}, \dots, r_{T,n_T})$ . If  $T$  has parent tables  $\text{Par}(T) = \{T_p^{(1)}, \dots, T_p^{(p)}\}$ , define for each row  $r_{T,k}$  the selected parent-row tuple

$$U_{T,k} = (u_{T,k}^{(1)}, \dots, u_{T,k}^{(p)}), \quad u_{T,k}^{(j)} \in \mathcal{V}(T_p^{(j)}).$$

For source tables (no FKs),  $U_{T,k}$  is taken to be empty. For a dependent table  $T$  with parents  $\text{Par}(T) = \{T_p^{(1)}, \dots, T_p^{(p)}\}$ , define the feasible parent-tuple set

$$\mathcal{C}_T := \mathcal{V}(T_p^{(1)}) \times \dots \times \mathcal{V}(T_p^{(p)}),$$

so that  $U_{T,k} \in \mathcal{C}_T$ . (For finite instances,  $\mathcal{C}_T$  is finite.)

**Assumption D.17** (Table Topological Order). There exists a topological ordering of tables  $\text{Topo}(G_S) = (T^{(1)}, \dots, T^{(N)})$  such that every foreign-key edge in  $G_S$  points from an earlier table to a later table.

Assumption D.17 implies a valid procedural generation order: parent tables can be sampled before child tables, and each dependent row selects parent rows and copies their PKs into FK cells. For a source table (no FKs), we generate its rows' latent states from exogenous noise. For a dependent table  $T_c$  with parent tables  $\text{Par}(T_c) = \{T_p^{(1)}, \dots, T_p^{(p)}\}$ , each new child row selects a tuple of parent rows  $(u^{(1)}, \dots, u^{(p)})$  and sets its FK values accordingly. This selection is the structural "routing" mechanism.

**Assumption D.18** (Structured Local Dependency). Fix a dependent table  $T$  with row order  $\pi_T = (r_{T,1}, \dots, r_{T,n_T})$  and parent tables  $\text{Par}(T) = \{T_p^{(1)}, \dots, T_p^{(p)}\}$ .

For each step  $k$ , let  $\mathcal{C}_{T,k} \subseteq \mathcal{C}_T$  be a finite candidate-tuple set, where  $\mathcal{C}_T = \mathcal{V}(T_p^{(1)}) \times \dots \times \mathcal{V}(T_p^{(p)})$ .

Define:

- **(Pre-selection context parents).** A set  $Pa^{ctx}(T, k)$  of structural cell instances drawn only from already-generated tables/rows (tables earlier than  $T$ , and rows  $\{r_{T,j}\}_{j < k}$  in  $T$ ), restricted to a bounded-hop neighborhood (radius  $k_0$ ) in the partially constructed instance graph.
- **(Candidate-local parents).** For each candidate tuple  $c \in \mathcal{C}_{T,k}$ , a set  $Pa^{cand}(c)$  of structural cell instances drawn from the rows in  $c$  and their bounded-hop neighborhoods (radius  $k_0$ ) in the partially constructed instance graph (again, only using already-generated variables).
- **(Embeddings).** A context embedding  $\text{Ctx}_{T,k} = \Phi_T^{ctx}(\{A_u\}_{u \in Pa^{ctx}(T,k)})$  and candidate embeddings  $\phi_{T,k}(c) = \Phi_T^{cand}(\{A_u\}_{u \in Pa^{cand}(c)})$ .

Let  $S_{T,k-1} = S(\{U_{T,j}\}_{j < k})$  be a permutation-invariant competition/degree summary of previous selections.

**(Markov restriction).** The local conditional depends on the past only through these pre-selection quantities:

$$P(U_{T,k}, Z_{r_{T,k}} \mid \text{all previously generated variables}) = P\left(U_{T,k}, Z_{r_{T,k}} \mid \text{Ctx}_{T,k}, \{\phi_{T,k}(c)\}_{c \in \mathcal{C}_{T,k}}, S_{T,k-1}\right).$$

For source tables, interpret  $U_{T,k}$ ,  $\mathcal{C}_{T,k}$ , and  $S_{T,k-1}$  as empty and keep only  $P(Z_{r_{T,k}} \mid \text{Ctx}_{T,k})$ .

**Assumption D.19** (Mechanism Sharing by Table/Relation Pattern). For each table  $T$ , all rows share the same conditional mechanism for producing  $(U_{T,k}, Z_{r_{T,k}})$  from their pre-selection inputs. Concretely, there exists a (table-specific) kernel  $K_T$  such that for all  $k$ ,

$$P\left(U_{T,k}, Z_{r_{T,k}} \mid \text{Ctx}_{T,k}, \{\phi_{T,k}(c)\}_{c \in \mathcal{C}_{T,k}}, S_{T,k-1}\right) = K_T\left(U_{T,k}, Z_{r_{T,k}} \mid \text{Ctx}_{T,k}, \{\phi_{T,k}(c)\}_{c \in \mathcal{C}_{T,k}}, S_{T,k-1}\right).$$

**Assumption D.20** (Hierarchy-Respecting Processing for Structure). The kernel  $K_T$  processes (i) the context parents  $Pa^{ctx}(T, k)$  and (ii) each candidate parent set  $Pa^{cand}(c)$  in a hierarchy-respecting way:

- **(Row-level order).** Within any row, structural cells (and optional row latents) are processed in a fixed canonical order.
- **(Within-table set invariance).** Within any table, sets of row representations are aggregated permutation-invariantly.
- **(Across-table order).** Tables are processed in a fixed canonical order (e.g., schema/topological order).
- **(Candidate-tuple role order).** Within a candidate tuple  $c = (u^{(1)}, \dots, u^{(p)})$ , the  $p$  parent roles are processed in the canonical FK-role order induced by the schema (so the tuple embedding is sensitive to role).
- **(Candidate-set symmetry).** The dependence of  $K_T$  on the candidate set  $\{\phi_{T,k}(c)\}_{c \in \mathcal{C}_{T,k}}$  is permutation-equivariant with respect to reordering candidates (e.g., implemented by scoring each candidate with a shared function and normalizing).

**Corollary D.21** (Stage 2 Factorization (Structure)). *Under Assumptions D.16, D.17, D.18, and D.19, the Stage 2 distribution admits an autoregressive factorization over tables and (within each table) rows:*

$$P(\{A_v\}_{v \in \mathcal{V}^{fk}}, \mathcal{Z} \mid G_S) = \prod_{T \in \text{Topo}(G_S)} \prod_{k=1}^{n_T} P\left(Z_{r_{T,k}}, U_{T,k} \mid \text{Ctx}_{T,k}, \{\phi_{T,k}(c)\}_{c \in \mathcal{C}_{T,k}}, S_{T,k-1}\right),$$

where  $U_{T,k}$ ,  $\mathcal{C}_{T,k}$  and  $S_{T,k-1}$  are empty for source tables.

*Proof.* Fix a topological table order  $\text{Topo}(G_S) = (T^{(1)}, \dots, T^{(N)})$  (Assumption D.17). For each table  $T^{(i)}$ , fix a row order  $\pi_{T^{(i)}} = (r_{T^{(i)},1}, \dots, r_{T^{(i)},n_i})$ . Under Assumption D.16, primary keys are deterministic, so the Stage 2 randomness is fully captured by

$$Y_{i,k} := (U_{T^{(i)},k}, Z_{r_{T^{(i)},k}}),$$

where  $U_{T^{(i)},k}$  is empty for source tables.

**Step 1 (Repeated chain rule over the nested order).** Applying the chain rule repeatedly over the nested order “tables then rows” gives

$$P(\{A_v\}_{v \in \mathcal{V}^{fk}}, \mathcal{Z} \mid G_S) = P(\{Y_{i,k}\}_{i,k} \mid G_S) = \prod_{i=1}^N \prod_{k=1}^{n_i} P(Y_{i,k} \mid G_S, \text{all variables generated before } (i, k)).$$

**Step 2 (Apply the candidate-based Markov restriction).** By Assumption D.18, for each dependent-table step  $(i, k)$  the conditional distribution of  $Y_{i,k} = (U_{T^{(i)},k}, Z_{r_{T^{(i)},k}})$  given all previously generated variables depends on the past only through: (i) the pre-selection context embedding  $\text{Ctx}_{T^{(i)},k}$ , (ii) the candidate set  $\mathcal{C}_{T^{(i)},k}$  and its candidate embeddings  $\{\phi_{T^{(i)},k}(c)\}_{c \in \mathcal{C}_{T^{(i)},k}}$ , and (iii) the within-table competition summary  $S_{T^{(i)},k-1} = S(\{U_{T^{(i)},j}\}_{j < k})$ . Hence,

$$P(Y_{i,k} \mid G_S, \text{all variables generated before } (i, k)) = P\left(Y_{i,k} \mid \text{Ctx}_{T^{(i)},k}, \{\phi_{T^{(i)},k}(c)\}_{c \in \mathcal{C}_{T^{(i)},k}}, S_{T^{(i)},k-1}\right),$$

with the convention that for source tables  $U_{T^{(i)},k}$ ,  $\mathcal{C}_{T^{(i)},k}$ , and  $S_{T^{(i)},k-1}$  are empty, so the right-hand side reduces to conditioning on  $\text{Ctx}_{T^{(i)},k}$  only.

**Step 3 (Substitute into the chain rule product).** Substituting the above identity into the product from Step 1 yields

$$P(\{A_v\}_{v \in \mathcal{V}^{fk}}, \mathcal{Z} \mid G_S) = \prod_{i=1}^N \prod_{k=1}^{n_i} P\left(Y_{i,k} \mid \text{Ctx}_{T^{(i)},k}, \{\phi_{T^{(i)},k}(c)\}_{c \in \mathcal{C}_{T^{(i)},k}}, S_{T^{(i)},k-1}\right),$$

which is exactly the claimed factorization after re-indexing  $(i, k)$  back to  $(T, k)$ .  $\square$

**A universal selective SCM.** We now give a constructive parameterization that can realize the Stage 2 factorization (Corollary D.21) while respecting Assumption D.20. Fix a dependent table  $T$  and row step  $k$  with candidate set  $\mathcal{C}_{T,k} \subseteq \mathcal{C}_T$  (in the idealized proof one may take  $\mathcal{C}_{T,k} = \mathcal{C}_T$ ).

For each row  $r_{T,k}$  we: (i) sample an initial latent  $Z_{r_{T,k}}^{(0)}$  from exogenous noise; (ii) compute a hierarchy-respecting *pre-selection* context embedding

$$z_{T,k}^{ctx} := \text{Ctx}_{T,k} = \Phi_T^{ctx}(\{A_u\}_{u \in P_{a^{ctx}}(T,k)});$$

(iii) compute candidate-tuple embeddings for each  $c \in \mathcal{C}_{T,k}$  by

$$\phi_{T,k}(c) = \Phi_T^{cand}(\{A_u\}_{u \in P_{a^{cand}}(c)});$$

(iv) score and sample a parent tuple  $U_{T,k} \in \mathcal{C}_{T,k}$  using a shared scoring function  $g$  and a uniform selector:

$$\ell_c = g\left(Z_{r_{T,k}}^{(0)}, z_{T,k}^{ctx}, \phi_{T,k}(c), S_{T,k-1}\right), \quad c \in \mathcal{C}_{T,k},$$

$$U_{T,k} = \text{Sample}(\text{Softmax}(\{\ell_c\}_{c \in \mathcal{C}_{T,k}}), U_{T,k}^{sel}), \quad U_{T,k}^{sel} \sim \text{Unif}(0, 1);$$

we then set the FK cell values of  $r_{T,k}$  to match the selected parent rows' PKs (referential integrity); and (v) update the latent state via a universal map  $\psi$ :

$$Z_{r_{T,k}} = \psi\left(Z_{r_{T,k}}^{(0)}, z_{T,k}^{ctx}, \phi_{T,k}(U_{T,k}), U_{T,k}^{lat}\right), \quad U_{T,k}^{lat} \sim \text{Unif}(0, 1),$$

where  $U_{T,k}^{lat}$  is independent noise.

For a source table  $T$  (no FKs), the mechanism omits the selection step and outputs

$$Z_{r_{T,k}} = \psi_T^{src}\left(\Phi_T^{ctx}(\{A_u\}_{u \in Pa^{ctx}(T,k)}), U_{T,k}^{lat}\right), \quad U_{T,k}^{lat} \sim \text{Unif}(0, 1),$$

with a table-shared map  $\psi_T^{src}$ .

**Theorem D.22** (Completeness of Stage 2 (Structure)). *Fix a schema  $G_S$ . Let  $P(\mathcal{D}_{struct}, \mathcal{Z} \mid G_S)$  be any structural distribution satisfying Assumptions D.16, D.17, D.18, D.19, D.20. Then there exists a parameter setting of the above selective SCM such that the induced distribution over  $(\mathcal{D}_{struct}, \mathcal{Z})$  approximates  $P(\mathcal{D}_{struct}, \mathcal{Z} \mid G_S)$  arbitrarily well in distribution.*

*Proof.* **Step 1 (Reduction to local kernels).** By Corollary D.21 (candidate-based factorization), it suffices to approximate each local conditional

$$P\left(Z_{r_{T,k}}, U_{T,k} \mid \text{Ctx}_{T,k}, \{\phi_{T,k}(c)\}_{c \in \mathcal{C}_{T,k}}, S_{T,k-1}\right),$$

with the convention that for source tables  $U_{T,k}$ ,  $\mathcal{C}_{T,k}$ , and  $S_{T,k-1}$  are empty.

**Step 2 (Sampling representation + approximation transfer).** Fix a dependent table  $T$  and step  $k$ . Define the (pre-selection) input

$$X_{T,k} := \left(\text{Ctx}_{T,k}, \{\phi_{T,k}(c)\}_{c \in \mathcal{C}_{T,k}}, S_{T,k-1}\right), \quad Y_{T,k} := (U_{T,k}, Z_{r_{T,k}}).$$

Since  $\mathcal{C}_{T,k}$  is finite and  $Z_{r_{T,k}} \in \mathbb{R}^d$ , the product space  $\mathcal{C}_{T,k} \times \mathbb{R}^d$  is standard Borel. By Lemma D.5, there exists a measurable sampler  $f_T$  and an independent  $U_{T,k}^{(gen)} \sim \text{Unif}(0, 1)$  such that

$$(U_{T,k}, Z_{r_{T,k}}) \stackrel{d}{=} f_T(X_{T,k}, U_{T,k}^{(gen)}).$$

Thus, if our model class contains  $\hat{f}_T$  with  $\hat{f}_T(X_{T,k}, U_{T,k}^{(gen)}) \rightarrow f_T(X_{T,k}, U_{T,k}^{(gen)})$  in probability under the induced input law, then the induced conditional law converges in distribution.

**Step 3 (Realizability by the structural SCM parameterization).** Write the target local kernel as

$$P(U_{T,k}, Z_{r_{T,k}} \mid X_{T,k}) = P(U_{T,k} \mid X_{T,k}) \cdot P(Z_{r_{T,k}} \mid X_{T,k}, U_{T,k}).$$

Because  $\mathcal{C}_{T,k}$  is finite, any categorical distribution  $P(U_{T,k} \mid X_{T,k})$  can be represented by logits  $\{\ell_c(X_{T,k})\}_{c \in \mathcal{C}_{T,k}}$  via

$$P(U_{T,k} = c \mid X_{T,k}) = \text{Softmax}(\{\ell_{c'}(X_{T,k})\}_{c' \in \mathcal{C}_{T,k}})_c,$$

e.g., by taking  $\ell_c(X_{T,k}) = \log P(U_{T,k} = c \mid X_{T,k})$  (up to an additive constant). Choosing the scoring network  $g$  from a universal approximator class over its inputs and using the candidate embeddings  $\phi_{T,k}(c)$  yields arbitrarily accurate approximation of these logits under the induced input law.

Conditioned on  $(X_{T,k}, U_{T,k})$ , the latent distribution  $P(Z_{r_{T,k}} \mid X_{T,k}, U_{T,k})$  admits a measurable sampler from uniform noise by Lemma D.5. Choosing the update map  $\psi$  from a universal approximator class yields an arbitrarily accurate approximation of this sampler in probability under the induced input law.

Finally, Assumption D.20 restricts dependence on the structural information to hierarchy-respecting processing. Choosing  $\Phi_T^{ctx}$  and  $\Phi_T^{cand}$  from universal hierarchy-respecting function classes yields arbitrarily accurate approximations of  $\text{Ctx}_{T,k}$  and  $\phi_{T,k}(c)$  as required.

**Step 4 (Conclude).** Combining (i) approximation of the categorical selection kernel for  $U_{T,k}$  and (ii) approximation of the conditional sampler for  $Z_{r_{T,k}}$  yields a sequence of structural SCM parameters whose induced local conditionals converge in distribution. Substituting these approximations into the Stage 2 factorization and using independent per-step noise variables gives convergence of the induced Stage 2 distribution to the target.  $\square$

## D.3.3. UNIVERSALITY OF THE THREE-STAGE CONSTRUCTION

**Theorem D.23** (Universality of the three-stage construction). *Let  $\mathcal{P}_{RDB}$  be the family of relational database distributions  $P(\mathcal{D})$  that factorize as*

$$P(\mathcal{D}) = P(G_S) P(\mathcal{D}_{struct}, \mathcal{Z} \mid G_S) P(\mathcal{D}_{dep} \mid \mathcal{D}_{struct}, \mathcal{Z}, G_S),$$

*and satisfy the Stage 2 assumptions and Stage 3 assumptions stated above.*

*Assume: (i) the schema model family  $\{\hat{P}_{\theta_S}(G_S)\}$  is dense in distributions over finite schema DAGs; (ii) for each fixed schema  $G_S$ , the Stage 2 family  $\{\hat{P}_{\theta_2}(\mathcal{D}_{struct}, \mathcal{Z} \mid G_S)\}$  is dense in the admissible  $P(\mathcal{D}_{struct}, \mathcal{Z} \mid G_S)$ ; and (iii) for each fixed  $(G_S, \mathcal{D}_{struct}, \mathcal{Z})$ , the Stage 3 family  $\{\hat{P}_{\theta_3}(\mathcal{D}_{dep} \mid \mathcal{D}_{struct}, \mathcal{Z}, G_S)\}$  is dense in the admissible  $P(\mathcal{D}_{dep} \mid \mathcal{D}_{struct}, \mathcal{Z}, G_S)$ .*

*Then the composite family*

$$\hat{P}_\theta(\mathcal{D}) = \hat{P}_{\theta_S}(G_S) \hat{P}_{\theta_2}(\mathcal{D}_{struct}, \mathcal{Z} \mid G_S) \hat{P}_{\theta_3}(\mathcal{D}_{dep} \mid \mathcal{D}_{struct}, \mathcal{Z}, G_S)$$

*is dense in  $\mathcal{P}_{RDB}$  (in distribution).*

*Proof sketch.* Fix any target  $P \in \mathcal{P}_{RDB}$  and  $\varepsilon > 0$ .

Choose  $\theta_S$  so that  $\hat{P}_{\theta_S}(G_S) \Rightarrow P(G_S)$ . Next, for each fixed schema  $G_S$ , choose  $\theta_2(G_S)$  so that  $\hat{P}_{\theta_2(G_S)}(\mathcal{D}_{struct}, \mathcal{Z} \mid G_S) \Rightarrow P(\mathcal{D}_{struct}, \mathcal{Z} \mid G_S)$ . Finally, for each fixed  $(G_S, \mathcal{D}_{struct}, \mathcal{Z})$ , choose  $\theta_3(G_S, \mathcal{D}_{struct}, \mathcal{Z})$  so that  $\hat{P}_{\theta_3(G_S, \mathcal{D}_{struct}, \mathcal{Z})}(\mathcal{D}_{dep} \mid \mathcal{D}_{struct}, \mathcal{Z}, G_S) \Rightarrow P(\mathcal{D}_{dep} \mid \mathcal{D}_{struct}, \mathcal{Z}, G_S)$ .

The joint law is the iterated mixture

$$P(\mathcal{D}) = \int P(G_S) \int P(\mathcal{D}_{struct}, \mathcal{Z} \mid G_S) P(\mathcal{D}_{dep} \mid \mathcal{D}_{struct}, \mathcal{Z}, G_S),$$

and  $\hat{P}_\theta(\mathcal{D})$  is defined by the same iterated mixture with each factor replaced by its approximation. Since weak convergence is preserved under forming such mixtures on standard Borel spaces,  $\hat{P}_\theta(\mathcal{D}) \Rightarrow P(\mathcal{D})$ .  $\square$

## E. Raw Results

Relational In-Context Learning via Synthetic Pre-training with Structural Prior

Table 4. Raw Results for Context Size 64

Part 1: First 10 Datasets										
Model	Amazon Churn	Avs Repeater	Diginetica Ctr	Outbrain Small Ctr	Rel Amazon Item Churn	Rel Amazon User Churn	Rel Avito User Clicks	Rel Avito User Visits	Rel Event User Ignore	Rel Event User Repeat
Random Forest	0.6036	0.5115	0.5792	0.5073	0.6530	0.5628	0.5743	0.4824	0.7326	0.6032
XGBoost	0.5757	0.5049	0.5000	0.5109	0.6417	0.5505	0.4884	0.5357	0.7317	0.6279
AutoGluon	0.5818	0.5059	0.5000	0.5038	0.6516	0.5339	0.4979	0.5254	0.7169	0.6170
Mitra	0.5828	0.5143	0.6434	0.5054	0.6876	0.5228	0.5797	0.5041	0.7066	0.5668
TabPFNv2	0.6265	0.5168	0.6034	0.5047	0.7412	0.5902	0.5708	0.5042	0.7401	0.5877
TabPFNv2.5	0.5976	0.5161	0.6105	0.5066	0.7269	0.5973	0.5734	0.4814	0.7548	0.5979
TabPFNv2.5-1estimator	0.5660	0.5124	0.5859	0.5056	0.7223	0.5723	0.5634	0.4851	0.7350	0.6017
TabICLv1	0.6468	0.5105	0.5995	0.5066	0.7067	0.5754	0.5641	0.5039	0.7737	0.5486
TabICLv1.1	0.6215	0.5047	0.5707	0.5036	0.6793	0.5468	0.5601	0.5133	0.7219	0.5820
TabICLv1.1-1estimator	0.6276	0.4991	0.5270	0.5036	0.6669	0.5462	0.5642	0.5070	0.6961	0.5609
LimiX2m	0.6537	0.5144	0.6073	0.5076	0.7044	0.5699	0.5633	0.5159	0.7342	0.5889
LimiX16m	0.6234	0.5092	0.6277	0.5105	0.7243	0.5831	0.5802	0.4756	0.7392	0.5872
LimiX16m-1estimator	0.6170	0.5067	0.6495	0.5093	0.7112	0.5755	0.5792	0.4806	0.7315	0.5846
RDBPFN_single.table	0.6241	0.5007	0.6604	0.5064	0.5911	0.5374	0.5796	0.4684	0.6513	0.5054
RDBPFN	0.6286	0.5172	0.6028	0.5106	0.7006	0.5791	0.5674	0.5061	0.7342	0.6055

Part 2: Remaining 9 Datasets and Average										
Model	Rel F1 Driver Dnf	Rel F1 Driver Top3	Rel Hm User Churn	Rel Stack User Badge	Rel Stack User Engagement	Rel Trial Study Outcome	Retailrocket Cvr	Stackexchange Churn	Stackexchange Upvote	Average
Random Forest	0.7049	0.7709	0.6087	0.7719	0.7654	0.5101	0.6432	0.7763	0.8276	0.6415
XGBoost	0.6937	0.7733	0.5890	0.6722	0.6331	0.5293	0.5596	0.7186	0.8045	0.6127
AutoGluon	0.6653	0.7445	0.5735	0.5927	0.5383	0.5064	0.5075	0.6903	0.8251	0.5936
Mitra	0.7068	0.7793	0.5878	0.8105	0.8015	0.5212	0.6525	0.7858	0.8199	0.6463
TabPFNv2	0.6952	0.7836	0.6239	0.7804	0.7645	0.5403	0.6602	0.7819	0.8422	0.6557
TabPFNv2.5	0.6948	0.7734	0.6221	0.7941	0.7674	0.5418	0.6390	0.7960	0.8424	0.6544
TabPFNv2.5-1estimator	0.6967	0.7775	0.6091	0.7816	0.7595	0.5328	0.6415	0.7882	0.8387	0.6461
TabICLv1	0.6909	0.7778	0.6067	0.8083	0.7995	0.5261	0.6715	0.7970	0.8150	0.6541
TabICLv1.1	0.7141	0.7686	0.5893	0.8044	0.7875	0.5299	0.6659	0.7662	0.8151	0.6445
TabICLv1.1-1estimator	0.7151	0.7725	0.5846	0.7955	0.7768	0.5077	0.6369	0.7786	0.8049	0.6353
LimiX2m	0.6892	0.7767	0.6007	0.7959	0.7874	0.5371	0.6684	0.7997	0.8184	0.6544
LimiX16m	0.7069	0.7667	0.6084	0.8107	0.7890	0.5421	0.6786	0.7903	0.8387	0.6575
LimiX16m-1estimator	0.7026	0.7784	0.5975	0.7992	0.7790	0.5504	0.6622	0.7758	0.8382	0.6541
RDBPFN_single.table	0.6063	0.7581	0.5618	0.7619	0.7220	0.5212	0.6075	0.7544	0.7569	0.6145
RDBPFN	0.6932	0.7952	0.6073	0.7729	0.7599	0.5474	0.6503	0.7669	0.8367	0.6517

Table 5. Raw Results for Context Size 128

Part 1: First 10 Datasets										
Model	Amazon Churn	Avs Repeater	Diginetica Ctr	Outbrain Small Ctr	Rel Amazon Item Churn	Rel Amazon User Churn	Rel Avito User Clicks	Rel Avito User Visits	Rel Event User Ignore	Rel Event User Repeat
Random Forest	0.6030	0.5234	0.5400	0.5002	0.6953	0.5816	0.5578	0.4754	0.7445	0.5909
XGBoost	0.5801	0.5154	0.5486	0.4989	0.6814	0.5657	0.4905	0.5635	0.7731	0.6049
AutoGluon	0.6071	0.5137	0.4972	0.5082	0.6693	0.5741	0.4922	0.5477	0.7407	0.6012
Mitra	0.6421	0.5323	0.6481	0.4933	0.7274	0.5842	0.5576	0.5496	0.7209	0.6203
TabPFNv2	0.6609	0.5304	0.5929	0.5043	0.7563	0.6261	0.5782	0.5264	0.7753	0.6274
TabPFNv2.5	0.5854	0.5331	0.5831	0.5098	0.7558	0.6278	0.5788	0.5083	0.7805	0.6452
TabPFNv2.5-1estimator	0.5783	0.5250	0.5772	0.5074	0.7464	0.6231	0.5489	0.5277	0.7745	0.6457
TabICLv1	0.6670	0.5209	0.6093	0.4957	0.7519	0.6141	0.5758	0.5199	0.7977	0.5498
TabICLv1.1	0.6426	0.5214	0.5729	0.5010	0.7431	0.5965	0.5588	0.5408	0.7577	0.5967
TabICLv1.1-1estimator	0.6476	0.5133	0.5243	0.4909	0.7358	0.5908	0.5623	0.5201	0.6989	0.6050
LimiX2m	0.6751	0.5320	0.5942	0.5045	0.7512	0.6122	0.5312	0.5603	0.7632	0.5792
LimiX16m	0.6241	0.5259	0.6391	0.5083	0.7553	0.6205	0.5393	0.5400	0.7541	0.5709
LimiX16m-1estimator	0.6051	0.5204	0.6197	0.5069	0.7496	0.6178	0.5361	0.5351	0.7519	0.5839
RDBPFN_single.table	0.6675	0.5105	0.6351	0.5019	0.6228	0.5761	0.5219	0.5252	0.6591	0.5317
RDBPFN	0.6408	0.5329	0.6398	0.4957	0.7532	0.6007	0.5605	0.5572	0.7486	0.6455

Part 2: Remaining 9 Datasets and Average										
Model	Rel F1 Driver Dnf	Rel F1 Driver Top3	Rel Hm User Churn	Rel Stack User Badge	Rel Stack User Engagement	Rel Trial Study Outcome	Retailrocket Cvr	Stackexchange Churn	Stackexchange Upvote	Average
Random Forest	0.6999	0.7822	0.6023	0.7595	0.7943	0.5340	0.7082	0.7853	0.8398	0.6483
XGBoost	0.6757	0.7824	0.5871	0.6454	0.7275	0.5379	0.6103	0.7383	0.8171	0.6286
AutoGluon	0.6932	0.7268	0.5604	0.5954	0.6289	0.5225	0.5588	0.6899	0.8341	0.6085
Mitra	0.7125	0.7936	0.5953	0.7794	0.7815	0.5273	0.7268	0.7766	0.8401	0.6636
TabPFNv2	0.6966	0.7907	0.6310	0.7569	0.7356	0.5488	0.7091	0.8018	0.8426	0.6680
TabPFNv2.5	0.6945	0.7924	0.6284	0.7569	0.7507	0.5519	0.7034	0.8179	0.8455	0.6658
TabPFNv2.5-1estimator	0.6985	0.7840	0.6184	0.7404	0.7425	0.5595	0.7030	0.8006	0.8411	0.6601
TabICLv1	0.7019	0.7866	0.6174	0.7882	0.8105	0.5426	0.7079	0.8134	0.8434	0.6692
TabICLv1.1	0.7088	0.7936	0.6301	0.7974	0.7990	0.5440	0.7083	0.7986	0.8437	0.6661
TabICLv1.1-1estimator	0.7057	0.7916	0.6173	0.7927	0.7982	0.5311	0.6958	0.8072	0.8395	0.6562
LimiX2m	0.6946	0.7950	0.6214	0.7267	0.7789	0.5638	0.7087	0.8101	0.8419	0.6655
LimiX16m	0.6839	0.7827	0.6058	0.7624	0.7535	0.5624	0.7000	0.7895	0.8461	0.6625
LimiX16m-1estimator	0.6765	0.7812	0.5993	0.7606	0.7487	0.5642	0.6907	0.7802	0.8439	0.6564
RDBPFN_single.table	0.6242	0.7653	0.5732	0.7607	0.7385	0.5393	0.6618	0.7902	0.8395	0.6339
RDBPFN	0.7000	0.8013	0.6159	0.7464	0.7803	0.5386	0.7127	0.7952	0.8410	0.6688

Relational In-Context Learning via Synthetic Pre-training with Structural Prior

Table 6. Raw Results for Context Size 256

Part 1: First 10 Datasets										
Model	Amazon Churn	Avs Repeater	Diginetica Ctr	Outbrain Small Ctr	Rel Amazon Item Churn	Rel Amazon User Churn	Rel Avito User Clicks	Rel Avito User Visits	Rel Event User Ignore	Rel Event User Repeat
Random Forest	0.6230	0.5189	0.5826	0.5177	0.7135	0.5812	0.5728	0.5250	0.7709	0.6257
XGBoost	0.5992	0.5163	0.5697	0.5142	0.7056	0.5792	0.5063	0.5631	0.8075	0.6265
AutoGluon	0.6075	0.5246	0.5173	0.5055	0.7274	0.5683	0.5006	0.5868	0.7797	0.6122
Mitra	0.6864	0.5353	0.6576	0.5018	0.7639	0.6129	0.5498	0.5812	0.7670	0.6438
TabPFNv2	0.6972	0.5324	0.6422	0.5284	0.7691	0.6321	0.5856	0.6047	0.8209	0.6797
TabPFNv2.5	0.6653	0.5356	0.6292	0.5275	0.7727	0.6310	0.6131	0.5585	0.8191	0.6732
TabPFNv2.5-1estimator	0.6655	0.5274	0.6193	0.5259	0.7697	0.6275	0.5691	0.5760	0.8047	0.6504
TabICLv1	0.7000	0.5175	0.6341	0.5107	0.7727	0.6212	0.6051	0.5764	0.8145	0.5825
TabICLv1.1	0.6981	0.5147	0.5790	0.5197	0.7701	0.6119	0.5879	0.5910	0.7871	0.6304
TabICLv1.1-1estimator	0.7119	0.5082	0.5536	0.5152	0.7710	0.6040	0.5834	0.5700	0.7326	0.6507
LimiX2m	0.6990	0.5184	0.6441	0.5252	0.7681	0.6263	0.5453	0.5899	0.7948	0.6304
LimiX16m	0.6416	0.5179	0.6536	0.5280	0.7700	0.6338	0.5351	0.5965	0.7817	0.6239
LimiX16m-1estimator	0.6293	0.5168	0.6577	0.5267	0.7645	0.6331	0.5248	0.6029	0.7800	0.6268
RDBPFN_single.table	0.7134	0.5073	0.6595	0.5103	0.6624	0.5681	0.5712	0.5900	0.7443	0.5827
RDBPFN	0.6604	0.5264	0.6566	0.5290	0.7570	0.6103	0.5968	0.6247	0.8073	0.6629

Part 2: Remaining 9 Datasets and Average										
Model	Rel F1 Driver Dnf	Rel F1 Driver Top3	Rel Hm User Churn	Rel Stack User Badge	Rel Stack User Engagement	Rel Trial Study Outcome	Retailrocket Cvr	Stackexchange Churn	Stackexchange Upvote	Average
Random Forest	0.6941	0.7765	0.5787	0.7849	0.8279	0.5442	0.7063	0.7846	0.8364	0.6613
XGBoost	0.6728	0.7907	0.5696	0.7609	0.7819	0.5547	0.6717	0.7638	0.8310	0.6518
AutoGluon	0.6797	0.7898	0.5873	0.7046	0.7131	0.5542	0.5962	0.7517	0.8424	0.6394
Mitra	0.7075	0.8147	0.6337	0.8193	0.8337	0.5373	0.7148	0.8154	0.8463	0.6854
TabPFNv2	0.7113	0.7995	0.6466	0.7624	0.8153	0.5883	0.7510	0.8238	0.8473	0.6967
TabPFNv2.5	0.7135	0.8056	0.6468	0.7916	0.8254	0.5913	0.7447	0.8422	0.8496	0.6966
TabPFNv2.5-1estimator	0.7173	0.8038	0.6426	0.7630	0.8095	0.5677	0.7299	0.8306	0.8472	0.6867
TabICLv1	0.7107	0.7982	0.6318	0.8161	0.8412	0.5842	0.7232	0.8270	0.8502	0.6904
TabICLv1.1	0.7137	0.8056	0.6473	0.8181	0.8438	0.5667	0.7157	0.8054	0.8438	0.6868
TabICLv1.1-1estimator	0.7155	0.8044	0.6386	0.8095	0.8423	0.5500	0.7084	0.8130	0.8466	0.6805
LimiX2m	0.7004	0.8098	0.6337	0.7925	0.8295	0.5972	0.7298	0.8297	0.8421	0.6898
LimiX16m	0.6960	0.7955	0.6327	0.7909	0.8197	0.5864	0.7240	0.8232	0.8453	0.6840
LimiX16m-1estimator	0.6799	0.7853	0.6082	0.7691	0.8167	0.5879	0.6974	0.8159	0.8418	0.6771
RDBPFN_single.table	0.6126	0.8079	0.5980	0.7567	0.7614	0.5858	0.7203	0.8285	0.8442	0.6645
RDBPFN	0.7171	0.8090	0.6279	0.7864	0.8255	0.5844	0.7418	0.8233	0.8436	0.6942

Table 7. Raw Results for Context Size 512

Part 1: First 10 Datasets										
Model	Amazon Churn	Avs Repeater	Diginetica Ctr	Outbrain Small Ctr	Rel Amazon Item Churn	Rel Amazon User Churn	Rel Avito User Clicks	Rel Avito User Visits	Rel Event User Ignore	Rel Event User Repeat
Random Forest	0.6392	0.5277	0.6084	0.5174	0.7292	0.6064	0.6129	0.5016	0.7821	0.6919
XGBoost	0.6219	0.5289	0.6143	0.5105	0.7289	0.5978	0.5707	0.5799	0.8100	0.6939
AutoGluon	0.6479	0.5280	0.5475	0.5223	0.7278	0.6073	0.5666	0.5852	0.7750	0.6731
Mitra	0.7106	0.5467	0.6717	0.5056	0.7833	0.6405	0.5941	0.6005	0.7846	0.6980
TabPFNv2	0.7220	0.5457	0.6356	0.5257	0.7814	0.6440	0.6130	0.6234	0.8286	0.7125
TabPFNv2.5	0.6772	0.5503	0.6109	0.5302	0.7841	0.6402	0.6256	0.5702	0.8265	0.7113
TabPFNv2.5-1estimator	0.6471	0.5478	0.6138	0.5123	0.7789	0.6369	0.6081	0.5954	0.8201	0.7037
TabICLv1	0.7160	0.5487	0.6539	0.5114	0.7775	0.6441	0.6264	0.6137	0.8163	0.6392
TabICLv1.1	0.7213	0.5446	0.5995	0.5152	0.7767	0.6463	0.6123	0.6169	0.7953	0.6741
TabICLv1.1-1estimator	0.7306	0.5384	0.5544	0.5107	0.7788	0.6420	0.6077	0.6037	0.7458	0.6627
LimiX2m	0.7213	0.5508	0.6638	0.5251	0.7731	0.6405	0.6029	0.6068	0.8121	0.6920
LimiX16m	0.6499	0.5484	0.6845	0.5279	0.7779	0.6380	0.6040	0.6162	0.8079	0.6901
LimiX16m-1estimator	0.6467	0.5355	0.6747	0.5259	0.7700	0.6410	0.5937	0.6242	0.8085	0.6883
RDBPFN_single.table	0.7378	0.5300	0.6516	0.4719	0.6667	0.6070	0.6221	0.6142	0.7565	0.6572
RDBPFN	0.7040	0.5536	0.6735	0.5256	0.7758	0.6445	0.6113	0.6253	0.8207	0.7276

Part 2: Remaining 9 Datasets and Average										
Model	Rel F1 Driver Dnf	Rel F1 Driver Top3	Rel Hm User Churn	Rel Stack User Badge	Rel Stack User Engagement	Rel Trial Study Outcome	Retailrocket Cvr	Stackexchange Churn	Stackexchange Upvote	Average
Random Forest	0.6916	0.7661	0.6017	0.7687	0.8149	0.5599	0.7169	0.7922	0.8448	0.6723
XGBoost	0.6883	0.7866	0.5907	0.7579	0.7910	0.5781	0.7070	0.7757	0.8445	0.6725
AutoGluon	0.7057	0.7698	0.6043	0.7465	0.7649	0.5654	0.6522	0.7800	0.8483	0.6641
Mitra	0.7138	0.8040	0.6650	0.8202	0.8356	0.5255	0.7529	0.8180	0.8502	0.7011
TabPFNv2	0.7190	0.8001	0.6659	0.7546	0.8273	0.6011	0.7766	0.8436	0.8570	0.7093
TabPFNv2.5	0.7151	0.7994	0.6662	0.7684	0.8315	0.6013	0.7647	0.8514	0.8576	0.7043
TabPFNv2.5-1estimator	0.7115	0.7950	0.6630	0.7503	0.8236	0.5977	0.7500	0.8461	0.8558	0.6977
TabICLv1	0.7126	0.7933	0.6535	0.8187	0.8323	0.5984	0.7383	0.8312	0.8546	0.7042
TabICLv1.1	0.7176	0.7887	0.6600	0.8202	0.8296	0.5926	0.7388	0.8115	0.8536	0.7008
TabICLv1.1-1estimator	0.7180	0.7832	0.6568	0.8054	0.8257	0.5717	0.7312	0.8203	0.8524	0.6916
LimiX2m	0.7156	0.7968	0.6535	0.7993	0.8206	0.6173	0.7463	0.8376	0.8536	0.7068
LimiX16m	0.7110	0.7977	0.6479	0.7780	0.8180	0.5843	0.7419	0.8356	0.8546	0.7007
LimiX16m-1estimator	0.7093	0.7903	0.6231	0.7527	0.8185	0.5775	0.7387	0.8292	0.8524	0.6947
RDBPFN_single.table	0.6640	0.7937	0.6393	0.8181	0.7985	0.5961	0.7453	0.8465	0.8322	0.6868
RDBPFN	0.7219	0.8023	0.6536	0.7816	0.8246	0.5986	0.7554	0.8444	0.8496	0.7102

Table 8. Raw Results for Context Size 1024

Part 1: First 10 Datasets										
Model	Amazon Churn	Avs Repeater	Diginetica Ctr	Outbrain Small Ctr	Rel Amazon Item Churn	Rel Amazon User Churn	Rel Avito User Clicks	Rel Avito User Visits	Rel Event User Ignore	Rel Event User Repeat
Random Forest	0.6360	0.5289	0.6125	0.5183	0.7425	0.6124	0.5973	0.5169	0.7913	0.6807
XGBoost	0.6200	0.5319	0.6198	0.5127	0.7410	0.5969	0.5409	0.5932	0.8174	0.6947
AutoGluon	0.6749	0.5299	0.5953	0.5208	0.7537	0.5952	0.5373	0.5974	0.8101	0.7075
Mitra	0.7009	0.5618	0.6959	0.5020	0.7882	0.6417	0.5627	0.6395	0.8059	0.7159
TabPFNv2	0.7219	0.5529	0.7057	0.5379	0.7975	0.6481	0.6290	0.6417	0.8299	0.7185
TabPFNv2.5	0.6693	0.5549	0.6638	0.5383	0.7961	0.6447	0.6326	0.6173	0.8318	0.7313
TabPFNv2.5-1estimator	0.6380	0.5532	0.6631	0.5233	0.7898	0.6439	0.6113	0.6220	0.8301	0.7200
TabICLv1	0.7239	0.5547	0.6769	0.5210	0.7870	0.6492	0.6189	0.6377	0.8216	0.6818
TabICLv1.1	0.7278	0.5494	0.6326	0.5256	0.7892	0.6482	0.6176	0.6441	0.8085	0.7004
TabICLv1.1-1estimator	0.7399	0.5446	0.6042	0.5186	0.7883	0.6464	0.6130	0.6395	0.7521	0.6806
LimiX2m	0.7117	0.5534	0.7034	0.5357	0.7845	0.6430	0.6159	0.6395	0.8249	0.6930
LimiX16m	0.6496	0.5582	0.7116	0.5373	0.7894	0.6394	0.6141	0.6461	0.8213	0.7176
LimiX16m-1estimator	0.6487	0.5550	0.6894	0.5335	0.7860	0.6428	0.5931	0.6478	0.8212	0.7135
RDBPFN_single.table	0.7455	0.5388	0.6639	0.4760	0.6660	0.6115	0.6200	0.6364	0.7601	0.6738
RDBPFN	0.7179	0.5599	0.7004	0.5352	0.7821	0.6479	0.6266	0.6546	0.8273	0.7533

Part 2: Remaining 9 Datasets and Average										
Model	Rel F1 Driver Dnf	Rel F1 Driver Top3	Rel Hm User Churn	Rel Stack User Badge	Rel Stack User Engagement	Rel Trial Study Outcome	Retailrocket Cvr	Stackexchange Churn	Stackexchange Upvote	Average
Random Forest	0.6779	0.7689	0.6227	0.7801	0.8240	0.5715	0.7454	0.7952	0.8375	0.6768
XGBoost	0.6948	0.7791	0.6050	0.7566	0.8172	0.5885	0.7269	0.7937	0.8460	0.6777
AutoGluon	0.6874	0.7684	0.6368	0.7640	0.7501	0.5748	0.6864	0.8100	0.8454	0.6761
Mitra	0.7113	0.8274	0.6673	0.8235	0.8575	0.5624	0.7733	0.8334	0.8538	0.7118
TabPFNv2	0.7142	0.7962	0.6685	0.8157	0.8568	0.6045	0.7981	0.8538	0.8606	0.7238
TabPFNv2.5	0.7165	0.8042	0.6683	0.8208	0.8534	0.6258	0.7912	0.8588	0.8609	0.7200
TabPFNv2.5-1estimator	0.7200	0.7927	0.6652	0.7860	0.8466	0.6232	0.7792	0.8532	0.8608	0.7117
TabICLv1	0.7157	0.8082	0.6666	0.8291	0.8626	0.6198	0.7580	0.8441	0.8557	0.7175
TabICLv1.1	0.7174	0.8059	0.6660	0.8297	0.8539	0.6080	0.7653	0.8197	0.8576	0.7140
TabICLv1.1-1estimator	0.7155	0.7765	0.6642	0.8205	0.8517	0.5843	0.7533	0.8237	0.8572	0.7039
LimiX2m	0.7122	0.8021	0.6627	0.8148	0.8528	0.6260	0.7735	0.8493	0.8570	0.7187
LimiX16m	0.7154	0.8072	0.6607	0.8021	0.8429	0.6102	0.7738	0.8448	0.8610	0.7159
LimiX16m-1estimator	0.7114	0.8070	0.6456	0.7820	0.8299	0.6050	0.7720	0.8439	0.8586	0.7098
RDBPFN_single.table	0.7086	0.7997	0.6523	0.8228	0.8086	0.5963	0.7700	0.8498	0.8303	0.6963
RDBPFN	0.7188	0.8115	0.6648	0.8126	0.8655	0.6159	0.7708	0.8477	0.8527	0.7245

Table 9. Single-Table Benchmark Results

Part 1: First 12 Datasets												
Model	Bioresponse	Diabetes130us	Higgs	Magiclelescope	Miniboone	Albert	Bank Marketing	California	Compas Two Years	Covertypes	Covertypes (v2)	Credit
Random Forest	0.8256	0.5861	0.7307	0.9107	0.9620	0.6899	0.8579	0.9318	0.6547	0.8579	0.8222	0.8386
XGBoost	0.8300	0.5666	0.7329	0.9046	0.9703	0.6647	0.8432	0.9397	0.6470	0.8480	0.8147	0.8148
AutoGluon	0.8146	0.6159	0.7208	0.9078	0.9650	0.6845	0.8582	0.9355	0.7210	0.8459	0.8104	0.8455
Mitra	0.8083	0.6341	0.7525	0.9250	0.9735	0.6969	0.8708	0.9475	0.7302	0.8456	0.8252	0.8518
TabPFNv2	0.8210	0.6366	0.7627	0.9263	0.9761	0.7026	0.8701	0.9567	0.7297	0.8684	0.8427	0.8511
TabPFNv2.5	0.8367	0.6356	0.7644	0.9307	0.9779	0.7011	0.8687	0.9530	0.7291	0.8739	0.8426	0.8511
TabPFNv2.5-1estimator	0.8247	0.6331	0.7574	0.9305	0.9763	0.6942	0.8673	0.9487	0.7317	0.8676	0.8351	0.8537
TabICLv1	0.8362	0.6335	0.7548	0.9290	0.9759	0.7011	0.8673	0.9459	0.7284	0.8652	0.8347	0.8514
TabICLv1.1	0.8372	0.6344	0.7619	0.9274	0.9777	0.7023	0.8661	0.9480	0.7259	0.8717	0.8430	0.8507
TabICLv1.1-1estimator	0.8160	0.6351	0.7512	0.9269	0.9761	0.6959	0.8687	0.9466	0.7257	0.8678	0.8370	0.8522
LimiX2m	0.8374	0.6351	0.7600	0.9261	0.9742	0.6971	0.8745	0.9573	0.7306	0.8762	0.8438	0.8492
LimiX16m	0.8393	0.6313	0.7639	0.9313	0.9773	0.6980	0.8740	0.9580	0.7313	0.8829	0.8468	0.8533
LimiX16m-1estimator	0.8364	0.6292	0.7564	0.9250	0.9753	0.6896	0.8674	0.9555	0.7290	0.8796	0.8360	0.8496
RDBPFN_single.table	0.7582	0.6317	0.7348	0.9100	0.9647	0.6935	0.8675	0.9248	0.7205	0.8225	0.8185	0.8337
RDBPFN	0.8107	0.6277	0.7469	0.9125	0.9605	0.6979	0.8683	0.9358	0.7269	0.8498	0.8259	0.8454

Part 2: Remaining 11 Datasets and Average												
Model	Default of Credit Card Clients	Default of Credit Card Clients (Cat)	Electricity	Electricity (Cat)	Eye Movements	Eye Movements (Cat)	Heloc	House 16h	Jannis	Pol	Road Safety	Average
Random Forest	0.7578	0.7527	0.8789	0.8700	0.6046	0.6025	0.7783	0.9342	0.8152	0.9941	0.7999	0.8024
XGBoost	0.7388	0.7323	0.8850	0.8713	0.6011	0.5935	0.7613	0.9371	0.8152	0.9949	0.7897	0.7955
AutoGluon	0.7593	0.7607	0.8709	0.8659	0.5948	0.5832	0.7697	0.9318	0.8019	0.9943	0.7851	0.8019
Mitra	0.7686	0.7692	0.8767	0.8718	0.5944	0.5905	0.7862	0.9460	0.8272	0.9945	0.8035	0.8126
TabPFNv2	0.7731	0.7734	0.8928	0.8824	0.6205	0.6176	0.7939	0.9471	0.8325	0.9976	0.8364	0.8222
TabPFNv2.5	0.7730	0.7739	0.8731	0.8683	0.6223	0.6179	0.7925	0.9464	0.8352	0.9981	0.8371	0.8219
TabPFNv2.5-1estimator	0.7734	0.7721	0.8693	0.8617	0.6171	0.6156	0.7864	0.9454	0.8372	0.9974	0.8319	0.8186
TabICLv1	0.7720	0.7729	0.8676	0.8615	0.6069	0.5983	0.7900	0.9464	0.8212	0.9962	0.8226	0.8165
TabICLv1.1	0.7743	0.7756	0.8768	0.8701	0.6140	0.6018	0.7900	0.9473	0.8305	0.9951	0.8193	0.8192
TabICLv1.1-1estimator	0.7744	0.7757	0.8737	0.8672	0.6146	0.6083	0.7865	0.9466	0.8310	0.9953	0.8128	0.8168
LimiX2m	0.7755	0.7749	0.8960	0.8838	0.6369	0.6264	0.7911	0.9470	0.8378	0.9971	0.8263	0.8241
LimiX16m	0.7731	0.7716	0.9023	0.8945	0.6526	0.6426	0.7882	0.9481	0.8419	0.9975	0.8305	0.8274
LimiX16m-1estimator	0.7693	0.7665	0.9009	0.8949	0.6228	0.6189	0.7839	0.9446	0.8384	0.9969	0.8214	0.8212
RDBPFN_single.table	0.7678	0.7688	0.8473	0.8415	0.5781	0.5821	0.7868	0.9402	0.8156	0.9854	0.7987	0.7997
RDBPFN	0.7722	0.7704	0.8695	0.8648	0.6050	0.5962	0.7900	0.9423	0.8226	0.9880	0.7974	0.8099

Table 10. Efficiency and complexity comparison of baseline models. Total inference time is calculated as the cumulative time required to evaluate all 19 relational benchmark tasks using a fixed 500-shot context ( $N = 500$ ).

Model	Parameters (M)	Pretraining Data (M)	Inference Time (s)
<i>Our Model</i>			
<b>RDB-PFN</b>	<b>2.64</b>	<b>2</b>	<b>34</b>
<i>Tabular Foundation Models (Full / Ensemble)</i>			
TabICL v1.1	103	80	229
Mitra	72	45	164
TabPFN v2.5	40	Undisclosed	156
LimiX 16M	16	Undisclosed	101
<i>Tabular Foundation Models (Lite / Single-Estimator)</i>			
TabICL-Lite	103	80	36
TabPFN-Lite	40	Undisclosed	43
LimiX-Lite	16	Undisclosed	54
<i>Classical Baselines</i>			
AutoGluon	-	-	172
XGBoost	-	-	57
Random Forest	-	-	48